Journal of Saudi Chemical Society (2022) **26**, 101468

King Saud University

Journal of Saudi Chemical Society

www.ksu.edu.sa
www.sciencedirect.com

ORIGINAL ARTICLE

Design, synthesis, *in vitro* and *in silico* studies of naproxen derivatives as dual lipoxygenase and α-glucosidase inhibitors

Asma Sardar [a], Obaid-ur-Rahman Abid [a], Saima Daud [a], M. Fakhar-e-Alam [b], Muhammad Hussnain Siddique [c,*], Muhammad Ashraf [d], Wardah Shahid [d], Syeda Abida Ejaz [e], M. Atif [f], Shafiq Ahmad [g], Sulman Shafeeq [h,*], Muhammad Afzal [c]

[a] *Department of Chemistry, Hazara University, Mansehra 21300, Pakistan*
[b] *Department of Physics, GC University Faisalabad, 38000, Pakistan*
[c] *Departmant of Bioinformatics and Biotechnology, Government College University Faisalabad, Allama Iqbal Road, Faisalabad, Pakistan*
[d] *Institute of Chemistry, The Islamia University of Bahawalpur, Bahawalpur 63100, Pakistan*
[e] *Department of Pharmaceutical Chemistry, Faculty of Pharmacy, The Islamia University of Bahawalpur, Bahawalpur 63100, Pakistan*
[f] *Department of Physics and Astronomy, College of Science, King Saud University, Riyadh 11451 Saudi Arabia*
[g] *Industrial Engineering Department, College of Engineering, King Saud University, P.O. Box 800, Riyadh 11421, Saudi Arabia*
[h] *Department of Microbiology, Tumor and Cell Biology, Karolinska Institute, Stockholm, Sweden*

Received 31 January 2022; revised 19 March 2022; accepted 23 March 2022
Available online 1 April 2022

KEYWORDS

Naproxen;
Thiosemicarbazides;
Azoles;
15-LOX;
α-glucosidase;
Cytotoxicity;
ADME studies;
Molecular docking

Abstract A series of 28 novel naproxen derivatives (4a-f, 5a-f, 6a-d, 7a-f, and 8a-f) have been designed, synthesized, and characterized. The synthesized derivatives were assessed as dual inhibitors for 15-lipoxygenase (LOX) and α-glucosidase enzymes and checked for cytotoxicity and ADME studies. The inhibitory potential of naproxen derivatives for 15- LOX was checked through two different methods, the UV absorbance method and the Chemiluminescence method. The biological activities result revealed that through the UV absorbance method, compound 4f (IC_{50} 21. 31 ± 0.32 μM) was found potent among the series followed by compounds 4e (IC_{50} 36.53 ± 0.5 1 μM) and 4d (IC_{50} 49.62 ± 0.12 μM) against standard drug baicalein (IC_{50} 22.46 ± 1.32 μM) and quercetin (IC_{50} 2.34 ± 0.35 μM), while through chemiluminescence method tested compounds

* Corresponding authors.
E-mail addresses: mhs1049@gmail.com (M.H. Siddique), sulman.shafeeq@ki.se (S. Shafeeq).
Peer review under responsibility of King Saud University.

Production and hosting by Elsevier

https://doi.org/10.1016/j.jscs.2022.101468

showed significant 15-LOX inhibition at the range of IC_{50} 1.13 ± 0.62 μM −123.47 ± 0.37 μM. Among these compounds, 4e (IC_{50} 1.13 ± 0.62 μM), 5b (IC_{50} 1.19 ± 0.43 μM), 8c (IC_{50} 1.23 ± 0.35 μM) were found most potent inhibitors against quercetin (IC_{50} 4.86 ± 0.14 μM), and baicalein (IC_{50} 2.24 ± 0.13 μM). The chemiluminescence method was found more sensitive than the UV method to identify 15-LOX inhibitors. Interestingly all synthesized compounds showed significant α-glucosidase inhibitory activity (IC_{50} 1.0 ± 1.13 μM − 367.2 ± 1.23 μM) even better than the standard drug acarbose (IC_{50} 375.82 ± 1.76 μM), while compound 6c (IC_{50} 1.0 ± 1.13 μM) and 7c (IC_{50} 1.1 ± 1.17 μM) were found most potent compounds among the series even many folds better than the standard drug. The cell viability results showed that all compounds were less toxic, maintained cellular viability at the range of 99.8 ± 1.3% to 63.7 ± 1.5%. ADME and molecular docking studies supported drug-likeness and binding interactions of compounds with the targeted enzymes.

1. Introduction

Non-steroids anti-inflammatory drugs (NSAIDs) are a class of drugs commonly used to treat inflammatory disorders, including pain associated with arthritis [1,2]. They inhibit the cyclooxygenase enzymes (COXs) responsible for prostaglandin synthesis, which causes inflammation [3]. Naproxen (2-(6-methoxynaphthalen-2-yl) propanoic acid) is a propionic derivative, one of the most significant non-steroid anti-inflammatory drugs (NSAIDs) that have anti-inflammatory, analgesic, and anti-pyretic properties, commonly used in the treatment of joint diseases, such as rheumatoid arthritis, osteoarthritis and gout and also reduces back pain and fever [4]. In addition to anti-inflammatory and analgesic activity [5,6] literature study revealed about other biological activities like anticancer, antimicrobial, antibacterial, anti-Alzheimer, antifungal, antinociceptive, antioxidant, anti-urease, and α-glucosidase inhibitory activities [7–13]. Most of these biological activities are associated with COX-dependent mechanisms; however, literature study revealed that NSAIDs interact with membrane phospholipids in a COX-independent route that could involve in their biological activity. The structures of some NSAIDs derivatives with specific biological activities are given in Fig. 1.

Lipoxygenases (LOX EC 1.13.11.12) are a group of non-heme iron-containing enzymes that catalyze incorporation of molecular oxygen in polyunsaturated fatty acids having a *cis*-1,4-pentadiene structure like arachidonic acid and linoleic acid to related unsaturated hydroperoxides [14]. These enzymes are broadly distributed in plants, animals as well as in microorganisms [15]. Literature survey has shown that mainly soybean 15-LOX isoform has been used for different biochemical processes because of its similarity with mammalian LOXs that catalyzes arachidonic acid, linoleic acid, and other unsaturated fatty acids in the same way [16,17]. Lipoxygenase inhibitors are used as drugs to treat various disorders such as inflammation, cancer, and bronchial asthma [18,19].

Various methods including UV, Chemiluminescence, fluorescence and colorimetric method have been described for

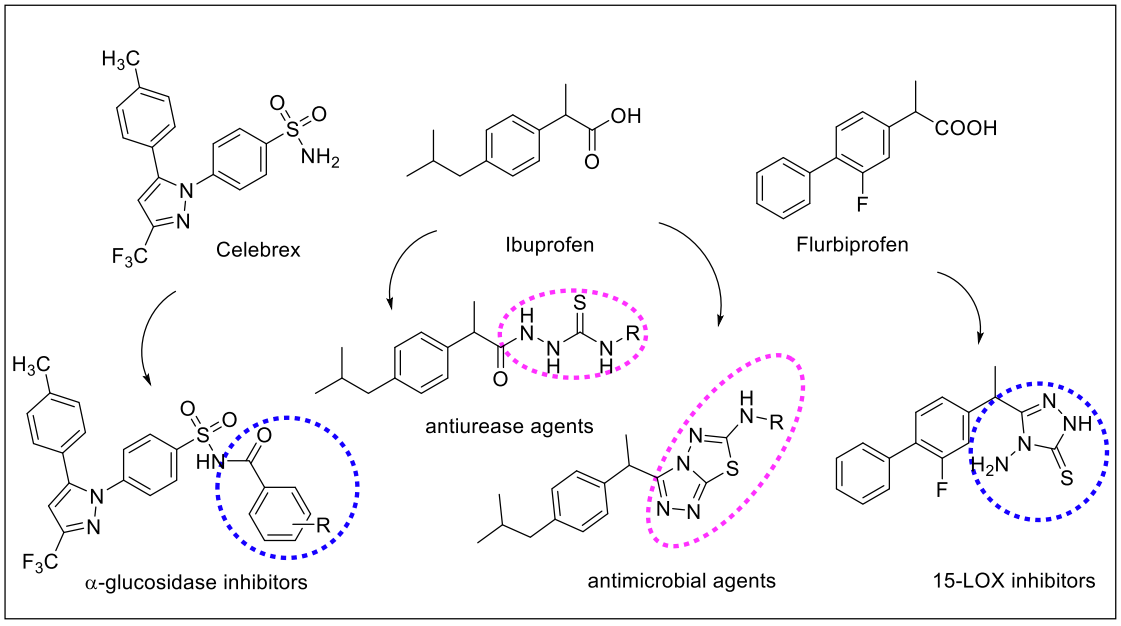

Fig. 1 Lead candidates derived from commercially available NSAIDs.

identifying LOX inhibitors [20]. The detection of the diene product generated via lipid peroxidation, 5(S)-hydroperoxy-6-*trans*-8,11,14-*cis*-eicosatetraenoic acid (HPETE) by the oxidation of linoleic acid as substrate at 234 nm, occurs in the UV absorbance method [21,22]. Chemiluminescence approach using luminol, a direct measurement of lipid hydroperoxide generated via LOX reaction, has also been reported, and improved with the addition of cytochrome *C* to the luminol mediated process. The reaction involves the formation of hydroperoxide from unsaturated fatty acids, which interacts with cytochrome *c* to produce oxygen radicals, which then oxidize luminol to its excited state, resulting in photon emissions recorded by the machine [23,24]. This method is a more sensitive and alternative way for detecting LOX activity. The fluorescent approach has also been used to study human 5-LOX inhibition [25,26]. The colorimetric method, which involves measuring the oxidation of the substrate and measuring the creation of colored compounds, produced unstable and fluctuating absorbance results. Lu et al. (2013) established a colorimetric approach in which lipid hydroperoxides produced from LOX oxidized ferrous ions to ferric ions, which then bonded thiocyanate ions to form a red ferric thiocyanate complex [27].

Diabetes mellitus type-II (DM-II) is a metabolic disorder and which is a chronic health problem all over the world. It is caused by a high level of blood glucose called hyperglycemia. Chronic hyperglycemia is associated with leading long-term complications of diabetes, obesity, metastatic cancer, and cardiovascular diseases [28]. Diabetes is a self-regulating risk factor of retinopathy, neuropathy, and nephropathy [29–31]. International Diabetic Federation (IDF), estimated that in 2019 approximately a 463 million adults (20–79 years) were living with diabetes; by 2045, this will rise to 700 million [32].

α-Glucosidase (EC. 3.2.1.20) is an exotype glycosidase enzyme that hydrolyze starch, and disaccharides into glucose. It is the key enzyme that is responsible for glucose absorption in the intestine [33], and is one of the validated therapeutic targets for drug design against hyperglycemia-related complications [34]. The various studies reported the relevance of α-glucosidase inhibition and regulation of glucose levels in DM-II by α-glucosidase inhibitors [35–37]. Several drugs like acarbose, miglitol, and voglibose are clinically used as α-glucosidase inhibitory anti-diabetic drugs in the last several decades, but these drugs also have some adverse effects such as constipation, abdominal pain, diarrhea, dizziness, vomiting, pneumatosis [38–40]. Therefore, there is a need of developing safer α-glucosidase inhibitors as anti-diabetic agents (Table 1).

Heterocycles are biologically essential scaffolds [41,42]. They have a crucial role in the various biochemical and pharmacological processes. Most of the naturally occurring compounds essential for living cells, such as essential amino acids, vitamins, coenzymes, sugars, etc., are all heterocyclic in nature [43]. These compounds played an essential role in medicinal chemistry, resulting in various therapeutic agents, with enhanced stability, reactivity, solubility, absorption, and bioavailability [44]. Among heterocyclic compounds, azoles moiety containing nitrogen, oxygen, and sulfur atoms received huge attention due to their broad spectrum of biological potential and vast therapeutic index [45–48]. Our research group has identified several heterocyclic compounds for their pharmacological potential [49–52]. Recently, we have reported some NSAIDs drugs including naproxen as 15-LOX inhibitors and ibuprofen derivatives as α-glucosidase inhibitors [53,54] Fig. 2]. However, further work is required to identify some promising lead molecules for future investigation.

In the present study, we report the synthesis of naproxen derivatives which were screened against two different enzymes i.e., 15-LOX and α-glucosidase to evaluate the enzyme inhibitory potential of these synthesized compounds. These derivatives were also screened for cell viability (cytotoxicity) and *in silico* studies were carried out in order to find binding interactions of naproxen derivatives with the said enzymes. To the best of our knowledge, this is the first report of the synthesized naproxen derivatives as 15-LOX and α-glucosidase inhibitors.

2. Experimental

2.1. Material and methods

All the reagents and chemicals were purchased from Sigma Aldrich which were used without additional purification. Naproxen was purchased from Alfa aesar. NMR (^{1}H NMR & ^{13}C NMR) spectra in deuterated solvent (DMSO d_6) were obtained on an Avance Bruker spectrometer at 400 MHz and 100 MHz. The coupling constants were expressed in hertz (Hz) and the chemical shift was reported in parts per million (ppm) with tetramethylsilane as an internal reference. Singlet (s), broad singlet (br s), doublet (d), doublet of doublet (dd),

Table 1 Structures of naproxen derivatives.

Comp.	X	R	Comp.	X	R
4a	—2F	–	**6c**	—4F	—$CH_2CH_2CH_3$
4b	—3F	–	**6d**	—3,4-diCl	—$CH_2CH_2CH_3$
4c	—4F	–	**7a**	—2F	–
4d	—2,3-diCl	–	**7b**	—3F	–
4e	—2,4-diCl	–	**7c**	—4F	–
4f	—3,4-diCl	–	**7d**	—2,3-diCl	–
5a	—2F	–	**7e**	—2,4-diCl	–
5b	—3F	–	**7f**	—3,4-diCl	–
5c	—4F	–	**8a**	—2F	–
5d	—2,3-diCl	–	**8b**	—3F	–
5e	—2,4-diCl	–	**8c**	—4F	–
5f	—3,4-diCl	–	**8d**	—2,3-diCl	–
6a	—4F	—CH_2CH_3	**8e**	—2,4-diCl	–
6b	—3,4-diCl	—CH_2CH_3	**8f**	—3,4-diCl	–

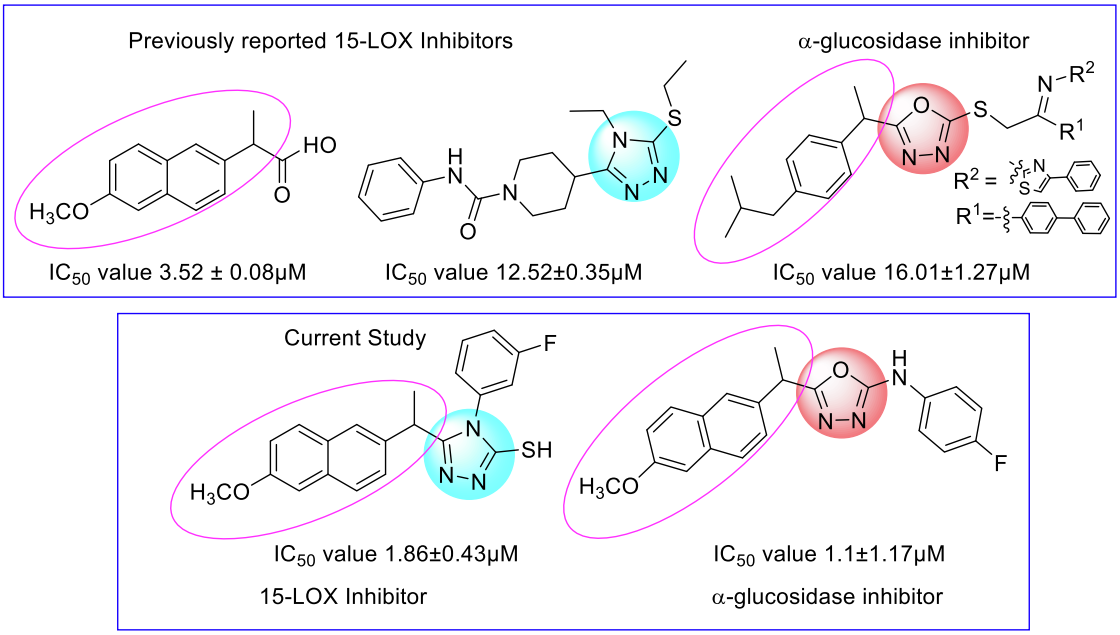

Fig. 2 The rationale of the study.

triplet (t), triplet of doublet (td), quartet (q), and multiplet (m) were reported as splitting patterns (m). A Finnegan MAT-311A mass spectrometer was used to record HRMS (EI) spectra. The melting points were obtained in an open capillary using the Stuart melting point device (SMP10). Thin layer chromatography with TLC plates precoated with silica gel 60 F_{254} was used to confirm all produced compounds.

2.2. General procedure for the synthesis of methyl 2-(6-methoxynaphthalen-2-yl) propanoate (2)

Naproxen methyl ester was synthesized by treating naproxen (0.01 mol) and dry methanol (20 mL) in the presence of few drops of conc. H_2SO_4, the reaction mixture, was refluxed for 7 hrs and monitored through TLC. After completion of reaction the excess solvent was evaporated and extracted through DCM and water (1:1.6) mixture to obtained solid product, which was dried and recrystallized from ethanol.

White solid; R_f = 0.71 (n-hexane: ethyl acetate 4:1); Yield 82%; m.p. 91-93℃. ^{1}H NMR (400 MHz, DMSO d_6) δ 7.64 (dd, J = 8.5, 2.1 Hz, 1H, Ar-H), 7.56 (dd, J = 8.8, 2.2 Hz, 1H, Ar-H), 7.47 (s, 1H, Ar-H), 7.39 (dd, J = 8.2, 2.0 Hz, 1H, Ar-H), 7.13 (d, J = 2.3 Hz, 1H, Ar-H), 6.92 (dd, J = 8.9, 2.5 Hz, 1H, Ar-H), 3.83 (s, 3H, OCH_3), 3.78 (q, J = 7.2 Hz, 1H, $\underline{CH}CH_3$), 3.62 (s, 3H, $CO\underline{CH_3}$), 1.49 (d, J = 7.2 Hz, 3H, $CH\underline{CH_3}$).^{13}C NMR (100 MHz, DMSO d_6) δ 174.4, 157.7, 137.4, 133.2, 129.2, 128.6, 127.3, 126.6, 125.3, 118.7, 105.6, 55.6, 51.9, 43.6, 18.5.

2.3. General procedure for the synthesis of 2-(6-methoxynaphthalen-2-yl)propane hydrazide (3)

A mixture of methyl 2-(6-methoxynaphthalen-2-yl) propanoate (0.01 mol) **(2)** and hydrazine hydrate (0.02 mol) was refluxed in ethanol (25 mL) for about 16 hrs. After completion of reaction the solid product was collected through filtrations, washed with water, dried, and recrystallized from ethanol. The reaction progress was monitored through TLC.

Brown solid; R_f = 0.18 (n-hexane: ethyl acetate 4:1); Yield 76%; m.p 138-140℃. ^{1}H NMR (400 MHz, DMSO d_6) δ 9.08 (s, 1H, NH), 7.69 (dd, J = 8.5, 2.1 Hz, 1H, Ar-H), 7.61 (dd, J = 8.0, 2.1 Hz, 1H, Ar-H), 7.49 (s, 1H, Ar-H), 7.39 (dd, J = 8.0, 2.2 Hz, 1H, Ar-H), 7.13 (d, J = 2.1 Hz, 1H, Ar-H), 6.92 (dd, J = 8.9, 2.5 Hz, 1H, Ar-H), 4.22(s, 2H, NH_2), 3.82 (s, 3H, OCH_3), 3.69 (q, J = 7.2 Hz, 1H, $\underline{CH}CH_3$), 1.45 (d, J = 7.4 Hz, 3H, $CH\underline{CH_3}$).^{13}C NMR (100 MHz, DMSO d_6) δ 176.4, 157.7, 139.8, 133.2, 129.1, 128.3, 127.2, 126.6, 125.2, 118.7, 105.6, 55.5, 44.9, 18.1.

2.4. General method for the synthesis of thiosemicarbazide derivatives 4(a-f)

An equimolar sum of 2-(6-methoxynaphthalen-2-yl) propane-hydrazide **(3)** (0.01 mol) and aryl isothiocyanate **(a-f)** was refluxed separately for 6–7 hrs in ethanol (25–30 mL) at 80℃. The progress of reaction was monitored through TLC. After completion of reaction, the reaction mixture was cooled at room temperature, the solvent was evaporated and solid left behind was washed and filtered to get the pure compound.

2.4.1. 4-(2-Fluorophenyl)-1-(2-(6-methoxynaphthalen-2-yl) propanoyl)thiosemicarbazide (4a)

Brown solid; R_f = 0.43 (n-hexane: ethyl acetate 4:1); Yield 72%; m.p. 151-153℃. ^{1}H NMR (400 MHz, DMSO d_6) δ 10.20 (br s, 1H, NH), 9.76 (br s., 1H, NH), 9.32 (br s, 1H, NH), 7.80–7.74 (m, 3H, Ar-H), 7.66 (d, J = 8.0 Hz, 1H, Ar-H), 7.52 (d, J = 8.0 Hz, 1H, Ar-H), 7.44 (d, J = 8.4 Hz, 1H, Ar-H), 7.35 (d, J = 2.4 Hz, 1H, Ar-H), 7.24–7.17 (m, 1H, Ar-H), 7.16 (s, 1H, Ar-H), 7.14 (dd, J = 8.8, 2.4 Hz, 1H, Ar-H), 4.03 (q, J = 6.8 Hz, 1H, $\underline{CH}CH_3$), 3.85 (s, 3H,

OCH_3), 1.48 (d, J = 7.2 Hz, 3H, CH_3). ^{13}C NMR (100 MHz, DMSO d_6) δ 181.8, 173.6, 157.7, 155.8 (d, J_{FC} = 245.4 Hz, C), 139.9, 133.2, 129.1, 128.4 (d, J_{FC} = 14.5 Hz, C), 128.1, 127.3, 126.6, 125.3, 124.8 (d, J_{FC} = 3.2 Hz, CH), 123.8 (d, J_{FC} = 7.3-Hz, CH), 122.5 (d, J_{FC} = 5.7 Hz, CH), 118.7, 115.5 (d, J_{FC} = 21.4 Hz, CH), 105.6, 55.6, 45.1, 18.1. HRMS (EI) calcd for $C_{21}H_{20}FN_3O_2S$ [M^+]: 397.1260 found 397.1247.

2.4.2. 4-(3-Fluorophenyl)-1-(2-(6-methoxynaphthalen-2-yl) propanoyl)thiosemicarbazide (4b)

Brown solid; R_f = 0.41 (n-hexane: ethyl acetate 4:1); Yield 76%; m.p. 149-151℃.^{1}H NMR (400 MHz, DMSO d_6) δ 10.17 (br s, 1H, NH), 9.56 (br s, 1H, NH), 8.92 (br s, 1H, NH), 7.79–7.76 (m, 1H, Ar-H), 7.73 (d, J = 2.4 Hz, 1H, Ar-H), 7.65–7.56 (m, 2H, Ar-H), 7.49 (d, J = 8.4 Hz, 1H, Ar-H), 7.33 (d, J = 7.6 Hz, 1H, Ar-H), 7.28 (d, J = 2.4 Hz, 1H, Ar-H), 7.24–7.17 (m, 2H, Ar-H), 7.07 (dd, J = 9.0, 2.5 Hz, 1H, Ar-H), 4.05 (q, J = 6.8 Hz, 1H, CHCH$_3$), 3.86 (s, 3H, OCH_3), 1.48 (d, J = 7.0 Hz, 3H, CH_3). ^{13}C NMR (100 MHz, DMSO d_6) δ 180.7, 173.5, 162.1 (d, J_{FC} = 246.5 Hz, C), 157.7, 139.8, 139.6 (d, J_{FC} = 16.4 Hz, (C), 133.2 (C), 130.3 (d, J_{FC} = 10.1 Hz, CH), 129.1, 128.4, 127.3, 126.6, 125.3, 119.2, 118.7, 113.4 (d, J_{FC} = 24.2 Hz, CH), 111.0 (d, J_{FC} = 22.3 Hz, CH), 105.6, 55.6, 45.1, 18.1. HRMS (EI) calcd for $C_{21}H_{20}FN_3O_2S$ [M^+]: 397.1260 found 397.1247.

2.4.3. 4-(4-Fluorophenyl)-1-(2-(6-methoxynaphthalen-2-yl) propanoyl)thiosemicarbazide (4c)

Brown solid; R_f = 0.43 (n-hexane: ethyl acetate 4:1); Yield 84%; m.p. 151-153℃.^{1}H NMR (400 MHz, DMSO d_6) δ 10.01 (br s, 1H, NH), 9.47 (br s, 1H, NH), 8.96 (br s, 1H, NH), 7.76–7. 64 (m, 2H, Ar-H), 7.57–7.49 (m, 2H, Ar-H), 7.42 (d, J = 7.5 Hz, 1H, Ar-H), 7.35 (d, J = 7.5 Hz, 1H, Ar-H), 7.28 (d, J = 2.3 Hz, 1H, Ar-H), 7.14 (dd, J = 8.4, 2.4 Hz, 1H, Ar-H), 7.04 (s, 1H, Ar-H), 6.99 (dd, J = 8.0, 2.5 Hz, 1H, Ar-H), 4.15 (q, J = 6.4 Hz, 1H, CHCH$_3$), 3.86 (s, 3H, OCH_3), 1.49 (d, J = 7.2 Hz, 3H, CH_3). ^{13}C NMR (100 MHz, DMSO d_6) δ 180.0, 173.8, 161.1, 157.9 (d, J_{CF} = 246.3 Hz, C), 139.8, 135.8 (d, J_{CF} = 2.8 Hz, C), 133.2, 129.1, 128.4, 127.3, 126.6, 126.2 (d, J_{CF} = 9.0 Hz, 2CH), 125.3, 118.7, 116.7 (d, J_{CF} = 22.5 Hz, 2CH), 105.6, 55.6, 45.1, 18.1. HRMS (EI) calcd for $C_{21}H_{20}FN_3O_2S$ [M^+]: 397.1260 found 397.1247.

2.4.4. 4-(2,3-Dichlorophenyl)-1-(2-(6-methoxynaphthalen-2-yl)propanoyl) thiosemicarbazide (4d)

Brown solid; R_f = 0.45 (n-hexane: ethyl acetate 4:1); Yield 74%; m.p. 98-100℃. ^{1}H NMR (400 MHz, DMSO d_6) δ 10.26 (br s, 1H, NH), 9.85 (br s, 1H, NH), 9.45 (br s, 1H, NH), 7.84–7.65 (m, 3H, Ar-H), 7.42 (d, J = 7.6 Hz, 1H, Ar-H), 7.35 (d, J = 8.4 Hz, 1H, Ar-H), 7.28 (d, J = 2.3 Hz, 1H, Ar-H), 7.17–7.12 (m, 3H, Ar-H), 4.15 (q, J = 6.6 Hz, 1H, CHCH$_3$), 3.86 (s, 3H, OCH_3), 1.49 (d, J = 7.0 Hz, 3H, CH_3). ^{13}C NMR (100 MHz, DMSO d_6) δ 181.9, 172.9, 157.7, 139.8, 135.4, 133.2, 132.9, 129.1, 128.5, 127.9, 127.3, 126.6, 125.3, 124.5, 123.3, 119.2, 118.7, 105.6, 55.6, 45.1, 18.1. (CH_3). HRMS (EI) calcd for $C_{21}H_{19}Cl_2$ N_3O_2S [M^+]: 447.0575 found 447.0561.

2.4.5. 4-(2,4-Dichlorophenyl)-1-(2-(6-methoxynaphthalen-2-yl)propanoyl) thiosemicarbazide (4e)

Light brown solid, R_f = 0.44 (n-hexane: ethyl acetate 4:1); Yield 70%; m.p. 100-102℃. ^{1}H NMR (400 MHz, DMSO d_6) δ 10.71 (br s, 1H, NH), 9.95 (br s, 1H, NH), 8.99 (br s, 1H, NH), 7.83 (d, J = 2.4 Hz, 1H, Ar-H), 7.76–7.59 (m, 3H, Ar-H), 7.49 (d, J = 7.6 Hz, 1H, Ar-H), 7.40 (s, 1H, Ar-H), 7.30 (dd, J = 8.4, 1.7 Hz, 1H, Ar-H), 7.18 (s, 1H, Ar-H), 7.10 (dd, J = 6.8, 2.4 Hz, 1H, Ar-H), 4.12 (q, J = 7.0 Hz, 1H, CHCH$_3$), 3.82 (s, 3H, OCH_3), 1.47 (d, J = 5.9 Hz, 3H, CH_3). ^{13}C NMR (100 MHz, DMSO d_6) δ 182.0, 173.7, 157.7, 139.8, 134.5, 133.2, 129.3, 129.1, 128.7, 128.3, 128.1, 127.7, 127.2, 126.7, 126.5, 125.2, 118.7, 105.6, 55.5, 45.1, 18.1. (CH_3). HRMS (EI) calcd for $C_{21}H_{19}Cl_2$ N_3O_2S [M^+]: 447.0575 found 447.0561.

2.4.6. 4-(3,4-Dichlorophenyl)-1-(2-(6-methoxynaphthalen-2-yl)propanoyl) thiosemicarbazide (4f)

Brown solid; R_f = 0.46 (n-hexane: ethyl acetate 4:1); Yield 83%; m.p. 98-100℃. ^{1}H NMR (400 MHz, DMSO d_6) δ 10.75 (br s, 1H, NH), 9.98 (br s, 1H, NH), 9.33 (br s, 1H, NH), 7.86 (d, J = 1.9 Hz, 1H, Ar-H), 7.79–7.64 (m, 2H, Ar-H), 7.43 (d, J = 8.6 Hz, 1H, Ar-H), 7.36 (d, J = 7.5 Hz, 1H, Ar-H), 7.28–7.03 (m, 4H, Ar-H), 4.02 (q, J = 6.0 Hz, 1H, CHCH$_3$), 3.85(s, 3H, OCH_3), 1.49 (d, J = 6.8 Hz, 3H, CH_3).^{13}C NMR (100 MHz, DMSO d_6) δ 180.9, 173.7, 157.7, 140.1, 139.8, 133.2, 131.8, 129.1, 128.9, 128.4, 127.3, 126.6, 125.3, 124.8, 124.1, 119.1, 118.4, 105.6, 55.6, 45.1, 18.1. HRMS (EI) calcd for $C_{21}H_{19}Cl_2$ N_3O_2S [M^+]: 447.0575 found 447.0561.

2.5. General procedure for the synthesis of 1, 2, 4-triazole-3-thiol derivatives 5(a-f)

First, 5% NaOH solution was prepared through stirring, then took 30 mL of stirred NaOH solution and added thiosemicarbazides **(4a-f)** (0.0011 mol) portion wise. The reaction mixture was allowed to reflux for 3 to 4 hrs, monitored through TLC. After cooling the reaction mixture was filtered and the filtrate was acidified with 6 N HCl to pH 2–3. The precipitated solid was filtered, washed thoroughly with water and recrystallized with ethanol.

2.5.1. 4-(2-Fluorophenyl)-5-(1-(6-methoxynaphthalen-2-yl) ethyl)-4H-1,2,4-triazole-3-thiol (5a)

Off white solid; R_f = 0.56 (n-hexane: ethyl acetate 4:1); Yield 74%; m.p 115-117℃. ^{1}H NMR (400 MHz, DMSO d_6) δ 13.89 (s, 1H, SH), 7.76–7.69 (m, 2H, Ar-H), 7.54–7.44 (m, 2H, Ar-H), 7.40 (d, J = 8.0 Hz, 1H, Ar-H), 7.39 (d, J = 7.6 Hz, 1H, Ar-H), 7.36 (d, J = 1.5 Hz, 1H, Ar-H), 7.15 (d, J = 7.0 Hz, 1H, Ar-H), 7.13 (d, J = 2.6 Hz, 1H, Ar-H), 6.97 (dd, J = 7.5, 1.5 Hz, 1H, Ar-H), 4.13 (q, J = 7.0 Hz, 1H, CHCH$_3$), 3.85 (s, 3H, OCH_3), 1.59 (d, J = 7.4 Hz, 3H, CH_3). ^{13}C NMR (100 MHz, DMSO d_6) δ 168.9, 161.6 (d, J_{FC} = 245.0 Hz, CF), 157.5, 152.3, 141.0, 133.2, 130.6 (d, J_{FC} = 7.3 Hz, CH), 129.8 (d, J_{FC} = 5.3 Hz, CH), 129.1, 128.6, 127.4, 126.8, 125.7, 125.0 (d, J = 3.2 Hz, CH), 121.5

(d, J_{FC} = 19.7 Hz, C), 118.7, 117.2 (d, J_{FC} = 21.4 Hz, CH), 105.6, 55.6, 37.6, 17.7. HRMS (EI) calcd for $C_{21}H_{18}FN_3OS$ [M^+]: 379.1155 found 379.1139.

2.5.2. 4-(3-Fluorophenyl)-5-(1-(6-methoxynaphthalen-2-yl) ethyl)-4H-1,2,4-triazole-3-thiol (5b)

Off white solid; R_f = 0.53 (n-hexane: ethyl acetate 4:1); Yield 78%; m.p. 120-123°C. ^{1}H NMR (400 MHz, DMSO d_6) δ 13.93 (s, 1H, SH), 7.78–7.58 (m, 4H, Ar-H), 7.42 (d, J = 8.0 Hz, 1H, Ar-H), 7.39 (d, J = 7.6 Hz, 1H, Ar-H), 7.36 (s, 1H, Ar-H), 7.15 (d, J = 7.0 Hz, 1H, Ar-H), 7.10 (s, 1H, Ar-H), 6.97 (dd, J = 7. 5, 1.5 Hz, 1H, Ar-H), 4.13 (q, J = 7.0 Hz, 1H, CHCH$_3$), 3.79 (s, 3H, OCH$_3$), 1.59 (d, J = 7.6 Hz, 3H, CH$_3$). ^{13}C NMR (100 MHz, DMSO d_6) δ 168.6, 162.1 (d, J_{FC} = 246.7 Hz, C), 157.6, 151.6, 141.0, 136.4 (d, J_{FC} = 13.7-Hz, C), 133.2, 130.5 (d, J_{FC} = 10.1 Hz, CH), 129.1, 128.6, 127.4, 126.8, 126.0 (d, J_{FC} = 3.8 Hz, CH), 125.7, 118.7, 116.6 (d, J_{FC} = 24.0 Hz, CH), 116.3 (d, J_{FC} = 22.3 Hz, CH), 105.6, 55.6, 37.6, 17.7. HRMS (EI) calcd for $C_{21}H_{18}FN_3$-OS [M^+]: 379.1155 found 379.1139.

2.5.3. 4-(4-Fluorophenyl)-5-(1-(6-methoxynaphthalen-2-yl) ethyl)-4H-1,2,4-triazole-3-thiol (5c)

White solid; R_f = 0.57 (n-hexane: ethyl acetate 4:1); Yield 81%; m.p 117-119°C. ^{1}H NMR (400 MHz, DMSO d_6) δ 13.90 (s, 1H, SH), 7.72–7.61 (m, 2H, Ar-H), 7.53–7.36 (m, 4H, Ar-H), 7.24 (d, J = 2.4 Hz, 1H, Ar-H), 7.19 (s, 1H, Ar-H), 7.10 (dd, J = 8.9, 2.5 Hz, 1H, Ar-H), 6.98 (dd, J = 8.5, 1.8 Hz, 1H, Ar-H), 4.06 (q, J = 7.0 Hz, 1H, CHCH$_3$), 3.85 (s, 3H, OCH$_3$), 1.57 (d, J = 7.0 Hz, 3H, CH$_3$). ^{13}C NMR (100 MHz, DMSO d_6) δ 168.7, 161.8 (d, J_{FC} = 246.3 Hz, C), 156.9, 151.6, 141.0, 134.0 (d, J_{FC} = 3.1 Hz, C), 133.2, 129.7 (d, J_{FC} = 8.4 Hz, 2CH), 129.1, 128.6, 127.4, 126.8, 125.7, 118.7, 117.0 (d, J_{FC} = 22.5 Hz, 2CH), 105.6, 55.6, 37.6, 17.7. HRMS (EI) calcd for $C_{21}H_{18}FN_3OS$ [M^+]: 379.1155 found 379.1139.

2.5.4. 4-(2,3-Dichlorophenyl)-5-(1-(6-methoxynaphthalen-2-yl)ethyl)-4H-1,2,4-triazole-3-thiol (5d)

Off white solid; R_f = 0.61 (n-hexane: ethyl acetate 4:1); Yield 74%; m.p. 187-189°C. ^{1}H NMR (400 MHz, DMSO d_6) δ 13.93 (s, 1H, SH), 7.74–7.71 (m, 1H, Ar-H), 7.58 (t, J = 8.0 Hz, 1H, Ar-H), 7.54 (d, J = 8.8 Hz, 1H, Ar-H), 7.38 (d, J = 8.4 Hz, 1H, Ar-H), 7.22 (d, J = 2.0 Hz, 1H, Ar-H), 7.09 (dd, J = 8.8, 2.4 Hz, 1H, Ar-H), 7.01 (s, 1H, Ar-H), 6.95 (dd, J = 8.4, 1.6 Hz, 1H, Ar-H), 3.95 (q, J = 6.9 Hz, 1H, CHCH$_3$), 3.84 (s, 3H, OCH$_3$), 1.60 (d, J = 6.8 Hz, 3H, CH$_3$).^{13}C NMR (100 MHz, DMSO d_6) δ 168.8, 157.6, 152.3, 141.0, 134.6, 133.9, 133.4, 132.6, 131.3, 130.4, 129.7, 129.1, 128.6, 127.4, 126.8, 125.7, 118.7, 105.6, 55.6, 37.6, 17.7. HRMS (EI) calcd for $C_{21}H_{17}Cl_2$ N_3OS [M^+]: 429.0469 found 429.0456.

2.5.5. 4-(2,4-Dichlorophenyl)-5-(1-(6-methoxynaphthalen-2-yl)ethyl)-4H-1,2,4-triazole-3-thiol (5e)

Brown solid; R_f = 0.64 (n-hexane: ethyl acetate 4:1); Yield 76%; m.p. 186-188°C. ^{1}H NMR (400 MHz, DMSO d_6) δ 13.90 (s, 1H, SH), 7.78–7.56 (m, 3H, Ar-H), 7.35 (d, J = 8.4 Hz, 1H, Ar-H), 7.26 (d, J = 8.4 Hz, 1H, Ar-H), 7.19 (s, 1H, Ar-H), 7.10 (dd, J = 7.6, 2.0 Hz, 1H, Ar-H), 7.05 (d, J = 1.5 Hz, 1H, Ar-H), 6.97 (dd, J = 8.0, 1.5 Hz, 1H, Ar-H), 3.90 (q, J = 6.9 Hz, 1H, CHCH$_3$), 3.85 (s, 3H, OCH$_3$), 1.59 (d, J = 7.2 Hz, 3H, CH$_3$). ^{13}C NMR (100 MHz, DMSO d_6) δ 169.2, 157.5, 152.3, 141.0, 138.8, 133.2, 133.1, 129.1, 129.1, 128.6, 127.4, 127.1, 126.8, 125.7, 123.9, 123.6, 118.7, 105.6, 55.6, 37.6, 17.7. HRMS (EI) calcd for $C_{21}H_{17}Cl_2$ N_3OS [M^+]: 429.0469 found 429.0456.

2.5.6. 4-(3,4-Dichlorophenyl)-5-(1-(6-methoxynaphthalen-2-yl)ethyl)-4H-1,2,4-triazole-3-thiol (5f)

Brown solid; R_f = 0.63 (n-hexane: ethyl acetate 4:1); Yield 82%; m.p. 187-190°C. ^{1}H NMR (400 MHz, DMSO d_6) δ 13.97 (s, 1H, SH), 7.84 (d, J = 2.4 Hz, 1H, Ar-H), 7.73 (d, J = 8.4 Hz, 1H, Ar-H), 7.63 (d, J = 8.8 Hz, 1H, Ar-H), 7.46 (d, J = 8.7 Hz, 1H, Ar-H), 7.32 (d, J = 9.7 Hz, 1H, Ar-H), 7.24 (d, J = 2.3 Hz, 1H, Ar-H), 7.21 (s, 1H, Ar-H), 7.11 (dd, J = 8.9, 2.5 Hz, 1H, Ar-H), 7.01 (dd, J = 8.4, 1.7 Hz, 1H, Ar-H), 4.11 (q, J = 6.8 Hz, 1H, CHCH$_3$), 3.85 (s, 3H, OCH$_3$), 1.58 (d, J = 7.1 Hz, 3H, CH$_3$). ^{13}C NMR (100 MHz, DMSO d_6) δ 168.9, 157.7, 151.6, 141.0, 136.6, 133.2, 132.8, 130.6, 129.1, 128.6, 127.4, 126.8, 126.6, 125.7, 124.3, 122.8, 118.7, 105.6, 55.6, 37.6, 17.7. HRMS (EI) calcd for $C_{21}H_{17}Cl_2$ N_3OS [M^+]: 429.0469 found 429.0456.

2.6. General method for the synthesis of alkylthio-1,2,4-triazoles derivatives 6(a-d)

A mixture of 5-(2-(2,6-dichlorophenylamino)benzyl)-4-(Aryl)-4H-1,2,4-triazole-3-thiol (0.002 mol) and K_2CO_3 (0.0015 mol) in DMF (15–20 mL) was refluxed for about 30 min then added ethyl/propyl bromide (0.0021 mol) dropwise to reaction mixture and refluxed for 2–3 hrs at 80°C. After completion of reaction (monitored through TLC), the reaction mixture was cooled and poured into ice cold water, precipitates were filtered out, washed, dried and recrystalized with ethanol.

2.6.1. 3-(Ethylthio)-4-(4-fluorophenyl)-5-(1-(6-methoxynaphthalen-2-yl)ethyl)-4H-1,2,4-triazole (6a)

White solid; R_f = 0.65 (n-hexane: ethyl acetate 4:1); Yield 75%; m.p 144-146°C. ^{1}H NMR (400 MHz, DMSO d_6) δ 7.71–7.56 (m, 4H, Ar-H), 7.37–7.30 (m, 2H, Ar-H), 7.24 (d, J = 2.4 Hz, 1H, Ar-H), 7.19 (s, 1H, Ar-H), 7.11 (dd, J = 8.2, 2.4 Hz, 1H, Ar-H), 6.98 (dd, J = 8.4, 1.7 Hz, 1H, Ar-H), 4.06 (q, J = 6.97 Hz, 1H, CHCH$_3$), 3.85 (s, 3H, OCH$_3$), 2.99 (q, J = 6.3 Hz, 2H, CH$_2$CH$_3$), 1.56 (d, J = 5.2 Hz, 3H, CHCH$_3$), 1.30 (t, J = 6.4 Hz, 3H, CH$_2$CH$_3$). ^{13}C NMR (100 MHz, DMSO d_6) δ 163.7, 161.8 (d, J_{FC} = 246.3 Hz, CF), 157.7, 153.5, 141.0, 134.0 (d, J_{FC} = 3.2-Hz, C), 133.2, 129.8 (d, J_{FC} = 8.4 Hz, 2CH), 129.1, 128.6, 127.4, 126.8, 125.7, 118.7, 117.1 (d, J_{FC} = 22.5 Hz, 2CH), 105.6, 55.9, 37.6, 27.2, 17.7, 14.5. HRMS (EI) calcd for $C_{23}H_{22}F$ N_3OS [M^+]: 407.1468 found 407.1454.

2.6.2. 4-(3,4-Dichlorophenyl)-3-(ethylthio)-5-(1-(6-methoxynaphthalen-2-yl)ethyl)-4H-1,2,4-triazole (6b)

Brown solid; R_f = 0.66 (n-hexane: ethyl acetate 4:1); Yield 72%; m.p156-158°C. ^{1}H NMR (400 MHz, DMSO d_6) δ 7.83 (d, J = 9.0 Hz, 1H, Ar-H), 7.72 (s, 1H, Ar-H), 7.62 (d, J = 8.0 Hz, 1H, Ar-H), 7.46 (d, J = 8.7 Hz, 1H, Ar-H), 7.32 (d, J = 9.7 Hz, 1H, Ar-H), 7.24 (d, J = 2.3 Hz, 1H, Ar-H), 7.21 (s, 1H, Ar-H), 7.11 (dd, J = 8.9, 2.5 Hz, 1H,

Ar-H), 7.00 (dd, J = 8.4, 1.6 Hz, 1H, Ar-H), 4.10 (q, J = 6.8 Hz, 1H, $\underline{CH}CH_3$), 3.85 (s, 3H, OCH_3), 2.99 (q, J = 6.8 Hz, 2H, $\underline{CH_2}CH_3$), 1.58 (d, J = 6.8 Hz, 3H, CH_3), 1.31 (t, J = 6.2 Hz, 3H, $CH_2\underline{CH_3}$). ^{13}C NMR (100 MHz, DMSO d_6) δ 162.1, 157.7, 153.6, 141.0, 136.7, 133.2, 133.0, 130.6, 129.1, 128.6, 127.4, 126.8, 126.5, 125.7, 124.7, 122.9, 118.7, 105.6, 55.6, 37.6, 27.2, 17.7, 14.5. HRMS (EI) calcd for $C_{23}H_{21}Cl_2N_3OS$ [M^+]: 457.0782 found 457.0769.

2.6.3. 4-(4-Fluorophenyl)-3-(1-(6-methoxynaphthalen-2-yl) ethyl)-5-(propylthio)-4H-1,2,4-triazole (6c)

White solid; R_f = 0.67 (n-hexane: ethyl acetate 4:1); Yield 76%; m.p. 139-141℃.^{1}H NMR (400 MHz, DMSO d_6) δ 7.76–7.65 (m, 2H, Ar-H), 7.51–7.46 (m, 2H, Ar-H), 7.40 (d, J = 8.4 Hz, 1H, Ar-H), 7.37 (d, J = 8.0 Hz, 1H, Ar-H) 7.24 (d, J = 2.44 Hz, 1H, Ar-H) 7.17 (d, J = 2.44 Hz, 1H, Ar-H) 7.12 (dd, J = 8.4, 1.7 Hz, 1H, Ar-H), 6.97 (dd, J = 7.8, 2.4 Hz, 1H, Ar-H), 4.03 (q, J = 6.9 Hz, 1H, $\underline{CH}CH_3$) 3.84 (s, 3H, OCH_3), 3.08 (t, J = 6.4 Hz, 2H, $\underline{CH_2}CH_2CH_3$), 1.57 (d, J = 7.2 Hz, 3H, $CH\underline{CH_3}$), 1.43–1.36 (m, 2H, CH_2 $\underline{CH_2}CH_3$), 0.99 (t, J = 7.2 Hz, 3H, $CH_2\underline{CH_3}$). ^{13}C NMR (100 MHz, DMSO d_6) δ 163.3, 161.8 (d, J_{FC} = 246.3 Hz, CF), 157.7, 153.6, 141.0, 134.0 (d, J_{FC} = 3.2 Hz, C), 133.2, 129.8 (d, J_{FC} = 8.4 Hz, 2CH), 129.1, 128.6, 127.4, 126.8, 125.7, 118.7, 117.1 (d, J = 22.5 Hz. 2CH), 105.64, 55.6, 37.6, 34.9, 24.5, 17.7, 12.5. HRMS (EI) calcd for $C_{24}H_{24}F$ N_3OS [M^+]: 421.1624 found 421.1611.

2.6.4. 4-(3,4-Dichlorophenyl)-3-(1-(6-methoxynaphthalen-2-yl)ethyl)-5-(propylthio)-4H-1, 2, 4-triazole (6d)

Whitish solid; R_f = 0.66 (n-hexane: ethyl acetate 4:1); Yield 71%; m.p. 150-152℃. ^{1}H NMR (400 MHz, DMSO d_6) δ 7.76 (d, J = 2.0 Hz, 1H, Ar-H), 7.74 (d, J = 7.4 Hz, 1H, Ar-H), 7.68 (d, J = 8.2 Hz, 1H, Ar-H), 7.46–7.32 (m, 2H, Ar-H), 7.24 (d, J = 2.3 Hz, 1H, Ar-H), 7.21–7.18 (m, 1H, Ar-H), 7.15 (d, 1H, Ar-H), 7.05 (dd, J = 8.0, 2.4 Hz, 1H, Ar-H), 4.11 (q, J = 6.8 Hz, 1H, $\underline{CH}CH_3$), 3.85 (s, 3H, OCH_3), 3.09 (t, J = 7.0 Hz, 2H, $\underline{CH_2}CH_2CH_3$), 1.61 (d, J = 6.7 Hz, 3H, $CH\underline{CH_3}$), 1.41–1.34 (m, 2H, $CH_2\underline{CH_2}CH_3$), 0.98 (t, J = 7.2 Hz, 3H, $CH_2\underline{CH_3}$). ^{13}C NMR (100 MHz, DMSO d_6) δ 161.6 157.7, 153.6, 141.0, 136.7, 133.2, 133.0, 130.6, 129.1, 128.6, 127.4, 126.8, 126.5, 125.7, 124.7, 122.9, 118.7, 105.6, 55.9, 37.6, 34.9, 24.5, 17.7, 12.5. HRMS (EI) calcd for $C_{24}H_{23}$-Cl_2N_3OS [M^+]: 471.0939 found 471.0927.

2.7. General method for the synthesis of 1, 3, 4-oxadiazole derivatives 7(a-f)

Oxadiazole derivatives **7(a-f)** were synthesized by the cyclization of thiosemicarbazides (0.001 mol) using mercuric acetate (0.0013 mol) in 10–15 mL ethanol as a solvent. The reaction mixture was refluxed for 2-3hrs with continuous stirring at 80℃. The progress of reaction was monitored through TLC. After completion of reaction, the solvent was evaporated and the product was recrystallized from ethanol and analyzed.

2.7.1. N-(2-Fluorophenyl)-5-(1-(6-methoxynaphthalen-2-yl) ethyl)-1,3,4-oxadiazol-2-amine (7a)

Brown solid; R_f = 0.55 (n-hexane: ethyl acetate 4:1); Yield 58%; m.p. 152-154℃. ^{1}H NMR (400 MHz, DMSO d_6) δ 10.16 (br s, 1H, NH), 8.04 (t, J = 7.8 Hz, 1H, Ar-H), 7.83–7.76 (m, 3H, Ar-H), 7.41 (dd, J = 8.4, 1.6 Hz, 1H, Ar-H), 7.31 (d, J = 2.0 Hz, 1H, Ar-H), 7.20–7.16 (m, 3H, Ar-H), 7.15–7.03 (m, 1H, Ar-H), 4.51 (q, J = 7.09 Hz, 1H, $\underline{CH}CH_3$), 3.81 (s, 3H, OCH_3), 1.70 (d, J = 7.0 Hz, 3H, CH_3).^{13}C NMR (100 MHz, DMSO d_6) δ 159.8, 157.7, 155.1 (d, J_{FC} = 245.4 Hz, C), 149.9, 139.9, 133.2, 129.1, 128.8, 128.6, 128.4 (d, J_{FC} = 14.5 Hz, C), 126.23, 126.0, 124.8 (d, J_{FC} = 3.4 Hz, CH), 123.8 (d, J_{FC} = 7.3 Hz, CH), 121.7 (d, J_{FC} = 5.7 Hz, CH), 118.7, 115.6 (d, J_{FC} = 21.4 Hz), 105.6, 55.6, 37.6, 16.1. HRMS (EI) calcd for $C_{21}H_{18}FN_3O_2$ [M^+]: 363.1383 found 363.1370.

2.7.2. N-(3-Fluorophenyl)-5-(1-(6-methoxynaphthalen-2-yl) ethyl)-1,3,4-oxadiazol-2-amine (7b)

Brown solid; R_f = 0.57(n-hexane: ethyl acetate 4:1); Yield 61%; m.p. 154-157℃. ^{1}H NMR (400 MHz, DMSO d_6) δ 10.16 (br s, 1H, NH), 7.91–7.66 (m, 4H, Ar-H), 7.41–7.13 (m, 6H, Ar-H), 4.53 (q, J = 6.05 Hz, 1H, $\underline{CH}CH_3$), 3.81 (s, 3H, OCH_3), 1.68 (d, J = 5.9 Hz, 3H, CH_3). ^{13}C NMR (100 MHz, DMSO d_6) δ 159.1, 157.6, 155.7 (d, J_{FC} = 246.5 Hz, C), 149.9, 140. 3 (d, J_{FC} = 16.6 Hz, C), 139.9, 133.2, 130.3 (d, J_{FC} = 10.1 Hz, CH), 129.1, 128.8, 128.6, 126.2, 126.0, 119.2 (d, J_{FC} = 3.4 Hz, CH), 118.7, 111.6 (d, J_{FC} = 24.2 Hz, CH), 111.01 (d, J_{FC} = 22.3 Hz, CH), 105.6, 55.9, 37.6, 16.2. HRMS (EI) calcd for $C_{21}H_{18}FN_3O_2$ [M^+]: 363.1383 found 363.1370.

2.7.3. N-(4-Fluorophenyl)-5-(1-(6-methoxynaphthalen-2-yl) ethyl)-1,3,4-oxadiazol-2-amine (7c)

Brown solid; R_f = 0.59 (n-hexane: ethyl acetate 4:1); Yield 70%; m.p. 156-158℃. ^{1}H NMR (400 MHz, DMSO d_6) δ 10.16 (br s, 1H, NH), 7.78–7.59 (m, 4H, Ar-H), 7.44 (d, J = 7.6, 1H, Ar-H), 7.32 (d, J = 7.4 Hz, 1H, Ar-H), 7.26–7.08 (m, 4H, Ar-H), 4.51 (q, J = 7.2 Hz, 1H, $\underline{CH}CH_3$), 3.80 (s, 3H, OCH_3), 1.71 (d, J = 6.4 Hz, 3H, CH_3). ^{13}C NMR (100 MHz, DMSO d_6) δ 159.1, 157.7, 155.5 (d, J_{FC} = 246.5 Hz, CF), 149.9, 139.9, 136.9 (d, J_{FC} = 2.7 Hz, C), 133.2, 129.1, 128.8, 128.6, 126.2, 126.0, 123.4 (d, J_{FC} = 8.8 Hz, 2CH), 118.7, 117.3 (d, J_{FC} = 22.5 Hz, 2CH), 105.6, 55.6, 37.6, 16.16. HRMS (EI) calcd for $C_{21}H_{18}FN_3O_2$ [M^+]: 363.1383 found 363.1370.

2.7.4. N-(2,3-Dichlorophenyl)-5-(1-(6-methoxynaphthalen-2-yl)ethyl)-1,3,4-oxadiazol-2-amine (7d)

Brown solid; R_f = 0.63 (n-hexane: ethyl acetate 4:1); Yield 76%; m.p. 127-130℃. ^{1}H NMR (400 MHz, DMSO d_6) δ 10.05 (br s, 1H, NH), 8.01 (d, J = 7.7 Hz, 1H, Ar-H), 7.84–7.73 (m, 3H, Ar-H), 7.41 (dd, J = 8.4, 1.5 Hz, 1H, Ar-H), 7.37–7.26 (m, 3H, Ar-H) 7.17 (dd, J = 8.8, 2.4 Hz, 1H, Ar-H) 4.51 (q, J = 7.2 Hz, 1H, $\underline{CH}CH_3$), 3.81 (s, 3H, OCH_3), 1.70 (d, J = 7.2 Hz, 3H, CH_3). ^{13}C NMR (100 MHz,

DMSO d_6) δ 160.2, 157.7, 149.9, 139.9, 135.8, 133.2, 132.6, 129.1, 128.8, 128.7, 128.6, 126.2, 126.0, 124.6, 123.1, 119.1, 118.7, 105.6, 55.6, 37.6, 16.2. HRMS (EI) calcd for $C_{21}H_{17}Cl_2N_3O_2$ [M^+]: 413.0698 found 413.0684.

2.7.5. N-(2,4-Dichlorophenyl)-5-(1-(6-methoxynaphthalen-2-yl)ethyl)-1,3,4-oxadiazol-2-amine (7e)

Light brown solid; R_f = 0.61 (n-hexane: ethyl acetate 4:1); Yield 56%; m.p. 124-126°C. ^{1}H NMR (400 MHz, DMSO d_6) δ 10.07 (br s, 1H, NH), 8.01 (d, J = 2.7 Hz, 1H, Ar-H) 7.74–7.65 (m, 2H, Ar-H), 7.41 (d, J = 8.4 Hz, 1H, Ar-H),7.38 (d, J = 8.0 Hz, 1H, Ar-H), 7.31–7.17 (m, 4H, Ar-H), 4.50 (q, J = 6.8 Hz, 1H, CHCH$_3$), 3.81 (s, 3H, OCH$_3$), 1.68 (d, J = 7.2 Hz, 3H, CH$_3$). ^{13}C NMR (100 MHz, DMSO d_6) δ 160.2, 157.7, 149.9, 139.9, 135.3, 133.2, 129.3, 129.1, 128.8, 128.7, 128.6, 128.5, 126.5, 126.2, 126.0, 125.8, 118.7, 105.6, 55.6, 37.6, 16.2. HRMS (EI) calcd for $C_{21}H_{17}Cl_2N_3O_2$ [M^+]: 413.0698 found 413.0684.

2.7.6. N-(3,4-Dichlorophenyl)-5-(1-(6-methoxynaphthalen-2-yl)ethyl)-1,3,4-oxadiazol-2-amine (7f)

Light brown solid; R_f = 0.61 (n-hexane: ethyl acetate 4:1); Yield 67%; m.p. 126-128°C. ^{1}H NMR (400 MHz, DMSO d_6) δ 10.03 (br s, 1H, NH), 7.96–7.65 (m, 3H, Ar-H) 7.46 (d, J = 8.2 Hz, 1H, Ar-H), 7.39 (d, J = 8.8 Hz, 1H, Ar-H) 7.23–7.09 (m, 4H, Ar-H), 4.53 (q, J = 6.8 Hz, 1H, CHCH$_3$) 3.80 (s, 3H, OCH$_3$), 1.68 (d, J = 5.8 Hz, 3H, CH$_3$). ^{13}C NMR (100 MHz, DMSO d_6) δ 159.1, 157.7, 149.9, 139.9, 139.7, 133.2, 131.7, 129.2, 128.9, 128.8, 128.6, 126.2, 126.0, 124.8, 122.1, 118.7, 118.4, 105.6, 55.6, 37.6, 16.2. HRMS (EI) calcd for $C_{21}H_{17}Cl_2N_3O_2$ [M^+]: 413.0698 found 413.0684.

2.8. General method for the synthesis of 1, 3, 4-Thiadiazoles derivatives 8(a-f)

A fine powder of the corresponding thiosemicarbazide **4(a-f)** (0.01 mol) was gradually added to concentrated sulphuric acid (5 mL, 0° C) separately and the reaction mixture was stirred for 1hr at 40° C. The reaction mixture was poured into crushed ice, filtered after melting of ice and then made the filtrate alkaline by ammonia solution to pH of 8. The product precipitate out and filtered. The filtered product was washed with cold water, dried and recrystallized with ethanol.

2.8.1. N-(2-Fluorophenyl)-5-(1-(6-methoxynaphthalen-2-yl) ethyl)-1,3,4-thiadiazol-2-amine (8a)

Brown solid; R_f = 0.54 (n-hexane: ethyl acetate 4:1); Yield 54%; m.p. 176-178°C. ^{1}H NMR (400 MHz, DMSO d_6) δ 9.72 (s, 1H, NH), 8.01–7.91 (m, 3H, Ar-H), 7.88–7.80 (m, 1H, Ar-H), 7.64 (dd, J = 8.4, 2.2 Hz, 1H, Ar-H), 7.59 – 7.51 (m, 1H, Ar-H), 7.41 (s, 1H, Ar-H), 7.29 (dd, J = 8.2, 1.8 Hz, 1H, Ar-H), 7.13 (d, J = 2.5 Hz, 1H, Ar-H), 7.00 (dd, J = 8.9, 2.5 Hz, 1H, Ar-H), 4.16 (q, J = 6.8 Hz, 1H, CHCH$_3$), 3.83 (s, 3H, OCH$_3$), 1.44 (d, J = 6.6 Hz, 3H, CH$_3$). ^{13}C NMR (100 MHz, DMSO d_6) δ 162.8, 158.2, 157.7, 155.8 (d, J_{FC} = 245.4 Hz, CF), 140.0, 133.2, 129.1, 128.6, 128.4 (d, J_{FC} = 14.7 Hz, C), 127.7, 127.3, 125.9, 125.0 (d, J_{FC} = 3.4 Hz, CH), 123.8 (d, J_{FC} = 7.2 Hz, CH), 122.7 (d, J_{FC} = 5.9 Hz, CH), 118.74, 115.7 (d, J_{FC} = 21.2 Hz, CH), 105.6, 55.6, 40.6, 18.5. HRMS (EI) calcd for $C_{21}H_{18}FN_3OS$ [M^+]: 379.1155 found 379.1141.

2.8.2. N-(3-Fluorophenyl)-5-(1-(6-methoxynaphthalen-2-yl) ethyl)-1,3,4-thiadiazol-2-amine (8b)

Brown solid; R_f = 0.59 (n-hexane: ethyl acetate 4:1); Yield 62%; m.p. 175-177°C. ^{1}H NMR (400 MHz, DMSO d_6) δ 10.25 (s, 1H, NH), 7.91–7.76 (m, 4H, Ar-H), 7.60 (dd, J = 8.0, 1.8 Hz, 1H, Ar-H), 7.51 (dd, J = 9.0, 3.1 Hz, 1H, Ar-H), 7.41 (d, J = 2.3 Hz, 1H, Ar-H), 7.29 (dd, J = 8.1, 1.9 Hz, 1H, Ar-H), 7.13 (d, J = 2.6 Hz, 1H, Ar-H), 7.03 (dd, J = 8.8, 2.4 Hz, 1H, Ar-H), 4.16 (q, J = 6.8 Hz, 1H, CHCH$_3$), 3.83 (s, 3H, OCH$_3$), 1.44 (d, J = 6.6 Hz, 3H, CH$_3$). ^{13}C NMR (100 MHz, DMSO d_6) δ 161.7, 159.9, 158.6 (d, J_{FC} = 246.7 Hz, CF), 156.9, 140.0, 139.7 (d, J_{FC} = 14.4 Hz, C), 133.2, 130.5 (d, J_{FC} = 10.1 Hz, CH), 129.1, 128.6, 127.7, 127.3, 125.9, 119.8 (d, J = 3.6 Hz, CH), 118.7, 112.7 (d, J_{CF} = 24.2 Hz, CH), 111.01 (d, J_{FC} = 22.3 Hz, CH), 105.6, 55.6, 40.6, 18.5. HRMS (EI) calcd for $C_{21}H_{18}FN_3OS$ [M^+]: 379.1155 found 379.1141.

2.8.3. N-(4-Fluorophenyl)-5-(1-(6-methoxynaphthalen-2-yl) ethyl)-1,3,4-thiadiazol-2-amine (8c)

Light brown solid; R_f = 0.57 (n-hexane: ethyl acetate 4:1); Yield 69%; m.p. 176-178°C. ^{1}H NMR (400 MHz, DMSO d_6) δ 10.25 (s, 1H, NH), 7.88–7.83 (m, 2H, Ar-H), 7.72–7.69 (m, 2H, Ar-H), 7.75 (dd, J = 8.2, 1.3 Hz, 1H, Ar-H), 7.53 (dd, J = 8.9, 2.0 Hz, 1H, Ar-H), 7.40 (dd, J = 3.6, 1.2 Hz, 1H, Ar-H), 7.29 (dd, J = 8.2, 1.8 Hz, 1H, Ar-H), 7.11 (d, J = 4.3 Hz, 1H, Ar-H), 6.88 (dd, J = 8.9, 2.4 Hz, 1H, Ar-H), 4.16 (q, J = 6.8 Hz, 1H, CHCH$_3$), 3.83 (s, 1H, OCH$_3$), 1.44 (d, J = 6.6 Hz, 1H, CH$_3$). ^{13}C NMR (100 MHz, DMSO d_6) δ 161.7, 158.1, 157.9 (d, J_{FC} = 246.3 Hz, C) 157.7, 140.0, 137.7 (d, J_{FC} = 2.8 Hz, C), 133.2, 129.2, 128.6, 127.7, 127.3, 125.9, 123.9 (d, J = 8.8 Hz, 2CH), 118.7, 117.4 (d, J_{FC} = 22.5 Hz, 2CH), 105.6, 55.6, 40.6, 18.5. HRMS (EI) calcd for $C_{21}H_{18}FN_3OS$ [M^+]: 379.1155 found 379.1141.

2.8.4. N-(2,3-Dichlorophenyl)-5-(1-(6-methoxynaphthalen-2-yl)ethyl)-1,3,4-thiadiazol-2-amine (8d)

Whitish solid; R_f = 0.62 (n-hexane: ethyl acetate 4:1); Yield 56%; m.p. 182-184°C. ^{1}H NMR (400 MHz, DMSO d_6) δ 9.83 (s, 1H, NH), 7.93 (dd, J = 7.9, 1.1 Hz, 1H, Ar-H), 7.85 (dd, J = 8.4, 2.2 Hz, 1H, Ar-H), 7.74 (t, J = 7.9 Hz, 1H, Ar-H), 7.60 (dd, J = 8.8, 1.8 Hz, 1H, Ar-H), 7.45 (dd, J = 7.9, 1.2 Hz, 1H, Ar-H), 7.36 (d, J = 1.7 Hz, 1H, Ar-H), 7.26 (dd, J = 8.2, 1.8 Hz, 1H, Ar-H), 7.13 (d, J = 2.6 Hz, 1H, Ar-H), 7.02 (dd, J = 8.4, 2.5 Hz, 1H, Ar-H), 4.16 (q, J = 6.8 Hz, 1H, CHCH$_3$), 3.83 (s, 3H, OCH$_3$), 1.44 (d, J = 6.6 Hz, 3H, CH$_3$). ^{13}C NMR (100 MHz, DMSO d_6) δ 162.7, 158.2, 157.7, 140.0, 135.7, 133.2, 133.1), 129.2, 128.8, 128.6, 127.7, 127.3, 125.9, 125.4, 123.1, 119.4, 118.7, 105.6, 55.6, 40.6, 18.5. HRMS (EI) calcd for $C_{21}H_{17}Cl_2N_3OS$ [M^+]: 429.0469 found 429.0453.

2.8.5. N-(2,4-Dichlorophenyl)-5-(1-(6-methoxynaphthalen-2-yl)ethyl)-1,3,4-thiadiazol-2-amine (8e)

Whitish solid; R_f = 0.60 (n-hexane: ethyl acetate 4:1); Yield 59%; m.p. 184-186°C. ^{1}H NMR (400 MHz, DMSO d_6) δ 9.96 (s, 1H, NH), 7.79 (d, J = 2.0 Hz, 1H, Ar-H), 7.75 – 7.69

(m, 2H, Ar-H), 7.56 (dd, J = 8.8, 2.4 Hz, 1H, Ar-H), 7.44 (dd, J = 8.4, 2.0 Hz, 1H, Ar-H), 7.30 (d, J = 2.0 Hz, 1H, Ar-H), 7.16 (dd, J = 8.0, 1.9 Hz, 1H, Ar-H), 7.06 (d, J = 1.9 Hz, 1H, Ar-H), 6.97 (dd, J = 8.9, 2.3 Hz, 1H, Ar-H), 4.16 (q, J = 7.3 Hz, 1H, $\underline{CH}CH_3$), 3.83 (s, 3H, OCH_3), 1.44 (d, J = 7.2 Hz, 3H, CH_3). ^{13}C NMR (100 MHz, DMSO d_6) δ 162.5, 158.0, 157.7, 140.0, 135.3, 133.2, 130.3, 129.2, 128.7, 128.6, 128.6, 127.7, 127.3, 126.6, 126.5, 125.9, 118.7, 105.6, 55.6, 40.6, 18.5. HRMS (EI) calcd for $C_{21}H_{17}Cl_2N_3OS$ [M^+]: 429.0469 found 429.0453.

2.8.6. N-(3,4-Dichlorophenyl)-5-(1-(6-methoxynaphthalen-2-yl)ethyl)-1,3,4-thiadiazol-2-amine (8f)

Whitish Peach solid; R_f = 0.63 (n-hexane: ethyl acetate 4:1); Yield 64%; m.p. 182-184℃. ^{1}H NMR (400 MHz, DMSO d_6) δ 10.25 (s, 1H, NH), 7.86–7.70 (m, 3H, Ar-H), 7.56 (dd, J = 8.0, 1.8 Hz, 1H, Ar-H), 7.45 (dd, J = 8.9, 1.7 Hz, 1H, Ar-H), 7.28 (d, J = 2.3 Hz, 1H, Ar-H), 7.20 (dd, J = 8.3, 1.9 Hz, 1H, Ar-H), 7.10 (d, J = 1.9 Hz, 1H, Ar-H), 7.02 (dd, J = 8.9, 2.5 Hz, 1H, Ar-H), 4.16 (q, J = 6.8 Hz, 1H, $\underline{CH}CH_3$), 3.83 (s, 3H, OCH_3), 1.44 (d, J = 6.6 Hz, 3H, CH_3). ^{13}C NMR (100 MHz, DMSO d_6) δ 161.7, 158.2, 157.7, 140.6, 140.0, 133.2, 131.7, 129.1, 128.8, 128.6, 127.7, 127.3, 125.9, 124.8, 123.7, 118.7, 118.6, 105.6, 55.6, 40.6, 18.5. HRMS (EI) calcd for $C_{21}H_{17}Cl_2N_3OS$ [M^+]: 429.0469 found 429.0453.

2.9. 15-LOX inhibition assay

2.9.1. UV absorbance method

The LOX assay was performed with minor changes as published earlier [50,55]. In a 96-well UV plate, a total of 200 μL of assay volume contained 100 mM phosphate buffer, 160 μL of pH 8.0, 10 μL of test compound, and 10 μL (210 units, following optimization of enzyme concentration) of 15-LOX. The components were mixed, and pre-incubated at 25℃ for 5 min before being measured at 234 nm using a BioTek HTX plate reader. The reaction was then started by adding 20 μL of linoleic acid substrate solution to each well. After 10 min of incubation, the change in absorbance was measured. In all assays, all reactions were performed in triplicates, and data is shown as mean with standard error of mean. The standard was quercetin / baicalein. The following formula was used to obtain the % inhibition.

$$Inhibition(\%) = (Abs\,of control - Abs\,of\,test\,comp/Abs\,of\,control) \times 100$$

The IC_{50} of the active compounds was calculated by determining their inhibition after suitable dilutions and data was computed using Ez-Fit Enzyme Kinetics software, Perrella Scientific Inc. Amherst, USA.

2.9.2. Chemiluminescence method

For the identification of inhibitors, a previously published chemiluminescence approach [56] was refined and employed. A total volume of 100 μL reaction mixture contained 60 μL borate buffer (200 mM, pH 9.0), 10 μL test substance or solvent, and 10 μL soybean LOX enzyme solution. This mixture was incubated in the dark for 5 min at 25 °C. The chemiluminescence was measured using a Bio Tek HTX 96 well plate reader in luminescence mode after adding 10 μL solution of luminol (3 nM) containing cytochrome c (1 nM) per well. The reaction was started by adding 10 μL of substrate solution as mentioned in UV absorbance method. Chemiluminescence was measured for 100 to 300 s. All reactions were performed in triplicates with both positive and negative controls. The percent inhibition and IC_{50} values were computed as mentioned above.

2.10. α-Glucosidase inhibition assay

For the synthesized derivatives, the α-glucosidase assay was carried out using Baker's yeast α–glucosidase (EC.3.2.1.20) and *p*-nitrophenyl-α-D-glucopyranoside [57]. The samples (5 μg/mL) were prepared by dissolving the synthesized compounds in DMSO. Test sample (10 μL) were prepared in 100 μL of phosphate buffer (100 mM) at pH 6.8 in 96-well microplate and incubated with 50 μL of Baker's yeast α-glucosidase for 5 min before 50 μL of p-nitrophenyl-α-D-glucopyranoside (5 mM) was added. After incubating for 5 min, the absorbance was measured spectrophotometrically at 405 nm. Blank in which substrate was changed with 50 mL of buffer were analyzed to accurately determine the background absorbance. Positive control sample (acarbose) was prepared containing 10 μL DMSO instead of test samples.

2.11. Cellular viability assay

From the healthy volunteer donor, 3 mL of fresh blood was taken. After that, the blood was diluted with phosphate buffer saline at a ratio of 1:1. In a 15 mL Falcon tube, an equivalent volume of lymphocyte separation medium (density 1.077 g/mL, at 20℃, Cat. No. L0560 Lymphosep, Biowest, USA) was added and poured onto the medium's surface. A swing rotor was used to centrifuge the contents at 1200 g for 20 min at 20℃. At the medium's interface, a ring of mononuclear cells MNCs was collected. The cells were collected and washed twice in 10 mL PBS 20 ℃ at 300 × g. The final pellet was then re-suspended in 0.5 mL PBS. RBCs and platelets were removed, and MNCs were washed in PBS to retain their entire volume and the requisite concentration of 20,000 per 10 μL was maintained in their total volume The number of MNCs produced a dose-dependent response that was linear in the tested range of 10–80 μL per well. With few adjustments, a previously published MTT assay technique was used [58]. In a 96-well plate, a known volume of PBS (50 mM, pH 7.4) was added to each well, followed by the addition of 10 μL test chemicals and 20 μL MNCs. At 37℃, the contents were incubated for 2 hrs. After the time period had passed, 10 μL of 0.25 mg/mL MTT solution was added to each well. In a 37℃ incubator, plates were incubated overnight for 18–20 hrs. Following the incubation period, 100 μL of DMSO was added to form a total volume of 200 μL. After 2 hrs, the absorbance was measured at 540 nm using a Synergy Bio Tek HTX plate reader. The triple assay contained both positive and negative controls. The following equation was used to calculate cell viability.

$$(Abs.\,of\,sample - Abs.\,of\,blank) \times 100 = cell\,viability\,(\%)$$

2.12. Molecular docking protocol

Molecular docking is a significant tool in drug discovery for acquiring the best possible pose in which a ligand binds to targeted receptor. In current studies, the best poses of docking were availed by utilizing commercial software Molecular Operating Environment (MOE, version 2015.10) [59–61]. Protein with PDB id: 3pzw (in case of 15-LOX) and PDB id:3Aj7.1.A (in case α-glucosidase; homology model was prepared by our group previously) [62] was taken from RCSB Protein Data Bank. Desired features of proteins were generated first. Forcefield MMFF94x loaded. Hetatoms and water molecules were removed. Polar Hydrogens and charges were incorporated. Then the database of ligands was created. Build dummies on amino acids of active pocket. Then docked the ligands with receptor/protein and total 10 poses were set for docking.

2.12.1. Visualization

The output files (results) were open in the MOE window and those poses were selected having minimum binding energy. The pose was best whose RMSD value was ≤ 2. Then visualize the interactions of ligand and protein.

3. Results and discussion

3.1. Chemistry

2-(6-Methoxynaphthalen-2-yl)propanehydrazide **3** was synthesized by the esterification of Naproxen **1** followed by the treatment of hydrazine hydrate in the presence of absolute ethanol. Furthermore, hydrazides **3** on treatment with various substituted aryl isothiocyanates gave thiosemicarbazides **4a-f.** Thiosemicarbazides were separately treated with 5% NaOH solution in the presence of ethanol to obtain 5-substituted-phenyl-4H-1,2,4-triazole-3-thiol **5a-f,** which was further treated with alkyl halides to get 5-substituted-phenyl-3-substituted S-4H-1,2,4-triazole **6a-d.** The thiosemicarbazides **4a-f** on further treatment with mercuric acetate in the presence of ethanol yielded 2-arylamino-5-substituted-1,3,4-oxadiazoles **7a-f** and that by stirring with cold sulphuric acid produced 2-arylamino-5-substituted-1,3,4-thiadiazoles **8a-f.** The synthesized compounds were evaluated based on their physical constants and spectral data like ^{1}H NMR, ^{13}C NMR data, which support the synthesis of all naproxen derivatives, are given in the experimental section. In general, in ^{1}H NMR spectra, the characteristics signals due to the NH (CONH, NHCSNH) protons appeared in the range of 10.75–8.92 ppm, confirms thiosemicarbazide **4a-f** synthesis, while in ^{13}C NMR spectra, the characteristics peaks of C = S and C = O appeared in the range of 182.0–180.0 ppm and 173.8–172.9 ppm respectively, strongly suggest compound **4a-f** synthesis. Further by the appearance of signals at 13.97–13.89 ppm strongly represent the SH group, and the disappearance of three NH peaks confirms the synthesis of compounds **5a-f**, while aromatic protons appeared in its relevant range. ^{13}C NMR also confirms the synthesis of compounds **5a-f** by the appearance of C-SH peak at 174.6–173.7 ppm. The disappearance of SH peak and the appearance of aliphatic protons attached with S group in the range of 3.09–0.98 ppm in ^{1}H NMR spectra and in ^{13}C

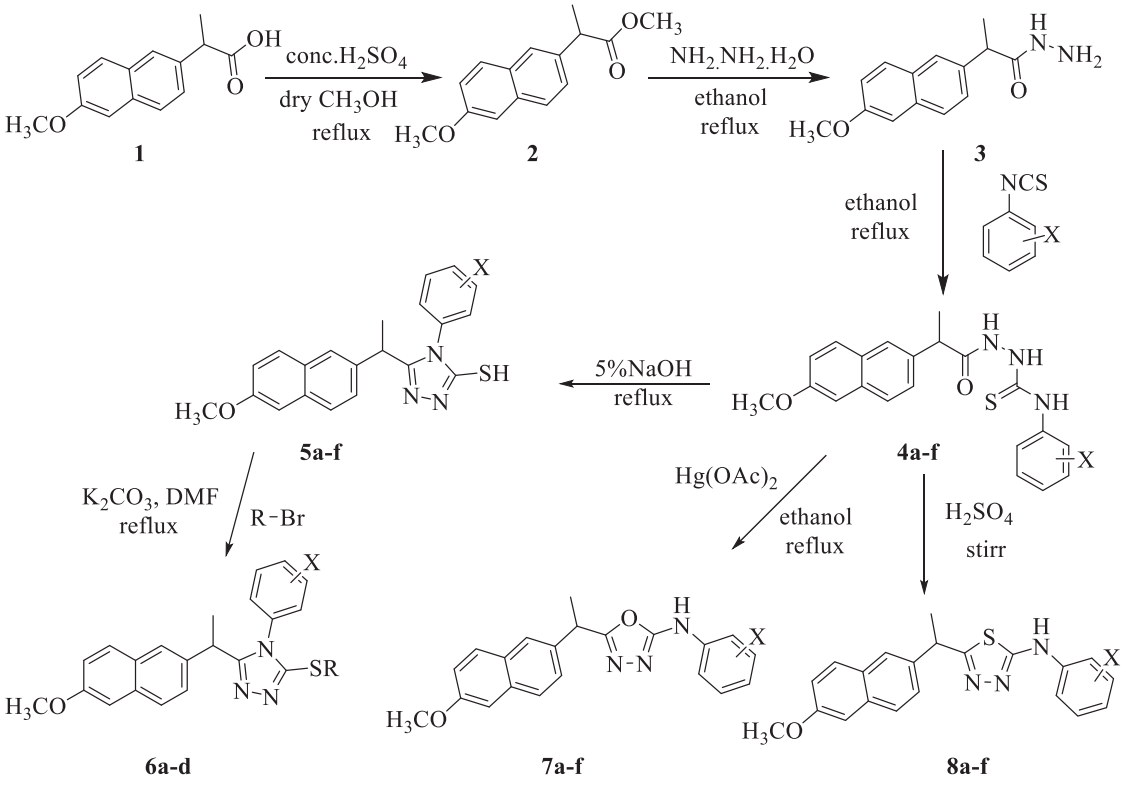

Scheme 1 Synthesis of naproxen derivatives.

NMR in the range of 37.6–12.5 ppm confirms compounds **6a-d** synthesis. As far as aromatic protons are concerned, they appear in their pertinent ranges. Synthesis of compounds **7a-f** and **8a-f** were also confirmed by ^{1}H NMR and ^{13}C NMR data. The appearance of NH proton in the range of 10.16–10.03 ppm and 10.25–9.72 ppm confirms the synthesis of compounds **7a-f** and **8a-f** respectively, while in ^{13}CNMR spectra, characteristic peak of C-NH of oxadiazole and thiadiazole ring appeared in the range of 160.2–159.1 ppm and 162.8–161.7 ppm, which confirmed the synthesis of oxadiazoles and thiadiazoles respectively. Further confirmation of all synthesized compounds was done by mass spectroscopic data. The synthetic scheme is illustrated in Scheme 1.

3.2. Biological evaluation

All the synthesized naproxen derivatives were screened for biological evaluation to find their inhibitory potential against 15-LOX and α-glucosidase enzymes. Our research group has identified some NSAIDs in our previous studies, including naproxen as 15-LOX inhibitors and ibuprofen derivatives as α-glucosidase inhibitors, with promising results [53,54]. These

Table 2 15-LOX, α-glucosidase inhibition and cell viability profile of naproxen derivatives.

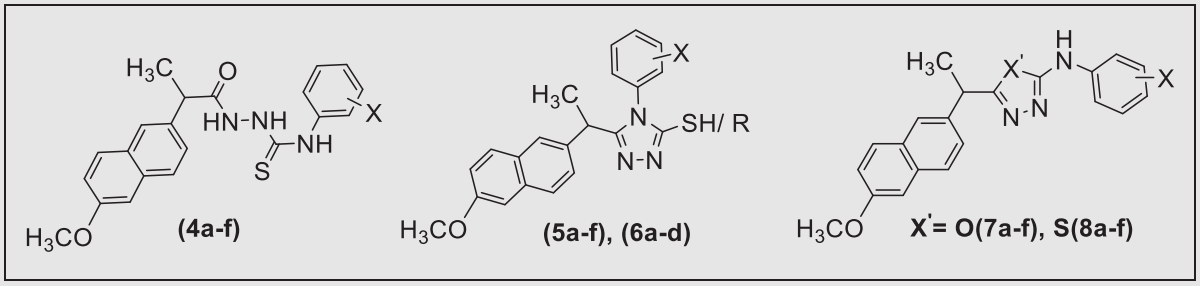

Compounds	IC_{50} (μM) ± SEM			Cell viability (%) at 0.25 mM
	15-LOX		α-Glucosidase	
	UV method	Chemiluminescence method		
4a	NA	NA	55.5 ± 1.12	87.2 ± 1.4
4b	NA	NA	161.1 ± 1.25	81.6 ± 1.6
4c	151.62 ± 0.32	22.31 ± 0.54	289.3 ± 1.13	80.5 ± 1.5
4d	49.62 ± 0.12	91.12 ± 0.48	121.6 ± 1.21	91.6 ± 1.6
4e	36.53 ± 0.51	1.13 ± 0.62	47.5 ± 1.17	99.8 ± 1.3
4f	21.31 ± 0.32	2.51 ± 0.71	67.3 ± 1.21	85.3 ± 1.5
5a	85.24 ± 0.35	2.61 ± 0.35	NA	96.2 ± 1.5
5b	67.41 ± 0.41	1.19 ± 0.43	186.5 ± 1.21	92.6 ± 1.8
5c	65.21 ± 0.26	2.13 ± 0.29	148.4 ± 1.17	95.3 ± 1.3
5d	64.36 ± 0.34	11.32 ± 0.35	211.6 ± 1.21	95.8 ± 1.4
5e	145.23 ± 0.42	12.44 ± 0.27	191.3 ± 1.12	96.4 ± 1.8
5f	> 250	12.84 ± 0.31	185.5 ± 1.11	94.3 ± 1.5
6a	> 250	104.25 ± 0.67	125.2 ± 1.17	89.7 ± 1.9
6b	73.45 ± 0.42	2.37 ± 0.35	340.14 ± 1.21	97.4 ± 1.7
6c	> 250	3.54 ± 0.56	1.01 ± 1.13	87.6 ± 1.3
6d	98.32 ± 0.51	98.43 ± 0.36	151.4 ± 1.21	95.4 ± 1.4
7a	NA	1.72 ± 0.54	121.3 ± 1.13	78.6 ± 1.6
7b	NA	31.67 ± 0.49	75.1 ± 1.12	73.6 ± 1.7
7c	213.41 ± 0.32	3.75 ± 0.65	1.1 ± 1.17	98.5 ± 1.8
7d	NA	42.85 ± 0.58	48.2 ± 1.21	63.7 ± 1.5
7e	NA	13.12 ± 0.41	2.1 ± 1.12	95.4 ± 1.3
7f	NA	42.66 ± 0.39	96.9 ± 1.11	65.4 ± 1.8
8a	NA	51.59 ± 0.28	359.3 ± 1.31	89.6 ± 1.7
8b	211.23 ± 0.29	NA	NA	89.3 ± 1.5
8c	65.21 ± 0.26	1.23 ± 0.35	24.3 ± 1.25	67.4 ± 1.2
8d	NA	3.45 ± 0.57	NA	81.2 ± 1.9
8e	NA	99.26 ± 0.45	367.2 ± 1.23	70.3 ± 1.6
8f	192.41 ± 0.34	123.47 ± 0.37	49.9 ± 1.47	68.6 ± 1.3
Quercetin	2.34 ± 0.35	4.86 ± 0.14	–	91.63 ± 1.4
Baicalein	22.46 ± 1.32	2.24 ± 0.13	–	Not tested
Cyclophosphamide	–	–	–	56.5 ± 1.8
Cisplatin	–	–	–	51.7 ± 1.9
Curcumin	–	–	–	73.9 ± 1.7
Acarbose	–	–	375.82 ± 1.76	–

Data is mean ± sem, n = 3, NA = Not Active.

findings encouraged us to explore naproxen derivatives biologically against these two enzymes. All the synthesized naproxen derivatives showed variant degrees of inhibitory potential against these two enzymes. Most of the compounds showed promising results in comparison to the previous study.

3.2.1. In vitro 15-LOX studies

The *in vitro* 15-LOX inhibitory studies of synthesized naproxen derivatives were determined by two different methods, i.e., UV absorbance method and chemiluminescence method. The results are depicted in Table 2. The inhibitory activity results obtained through the UV absorbance method showed that all the synthesized derivatives showed moderate to poor inhibition in comparison with quercetin (IC_{50} 2.34 ± 0.35 μM) and baicalein (IC_{50} 22.46 ± 1.32 μM) used as standard inhibitors except compounds **4a**, **4b**, **7a**, **7b**, **7d-f**, and **8a**, which were found inactive. Comparison of their bioactivity is as below:

Thiosemicarbazides **4a-f** were found as the most active (potent) inhibitors (IC_{50} values of 21.31 ± 0.32 to 151.62 ± 0.32 μM) among the synthesized derivatives. In this series, compound **4f** (IC_{50} 21.31 ± 0.32 μM) having dichloro group at 3,4 position was found the most potent compound among the series followed by compounds **4e** (IC_{50} 36.53 ± 0.51 μM) having dichloro group at 2,4 position and **4d** (IC_{50} 49.62 ± 0.12 μM) having dichloro group at 2,3 position. It means that in thiosemicarbazides, the dichloro substituted N-phenyl group enhanced the activity compared to the fluoro substituted N-phenyl group, which lowered the inhibition, while **4a** and **4b** were found to be inactive. 5-Substituted-phenyl-4H-1,2,4-triazole-3-thiols **5a-f** exhibited good to moderate (IC_{50} 64.36 ± 0.34 μM to 145.23 ± 0.42 μM) inhibitory profiles, while S-alkylated 1,2,4-triazoles **6a-d** showed moderate inhibition in which compound **6b** emerged with IC_{50} 73.45 ± 0.42 μM while all other compounds appeared with $IC_{50} > 250$ μM. 2-Arylamino-5-substituted 1,3,4-oxadiazoles **7a-f** were found inactive except compound **7c** (IC_{50} 213.41 ± 0.32 μM), which showed poor inhibition. 2-Arylamino-5-substituted-1,3,4-thiadiazoles **8a-f** exhibited moderate to poor inhibition (IC_{50} 65.21 ± 0.26 to 211.23 ± 0.29 μM) while compounds **8a**, **8c**, and **8d** were found inactive altogether.

Chemiluminescence method results suggest that this method is sensitive, fast, and better than the UV absorbance method. The general screening was done at 0.25 mM concentration. Quercetin (IC_{50} 4.86 ± 0.14 μM) and baicalein (IC_{50} 2.24 ± 0.13 μM) were used as standard inhibitors. The most potent inhibitors among the whole series were 5-substituted-phenyl-4H-1,2,4-triazole-3-thiols **5a-f** (IC_{50} 1.86 ± 0.43 to 12.84 ± 0.31 μM). In this series, the most active compounds were those having fluoro substituent at 2, 3, and 4 positions, respectively, i.e., **5a** (IC_{50} 2.61 ± 0.35 μM), **5b** (IC_{50} 1.19 ± 0.43 μM), and **5c** (IC_{50} 2.13 ± 0.29 μM), followed by triazoles dichloro groups at 2,3/ 2,4 and 3,4 position, i.e., **5d** (IC_{50} 11.32 ± 0.35 μM), **5e** (IC_{50}12.44 ± 0.27 μM, and **5f** (IC_{50} 12.84 ± 0.31 μM). S-Alkylated 1,2,4-triazoles **6a-d** were found least active in comparison to triazoles, except compound **6b** (IC_{50} 2.37 ± 0.35 μM), and **6c** (IC_{50} 3.54 ± 0.56 μM) that showed potent inhibition. 2-Arylamino-5-substituted 1,3,4-

Table 3 ADME properties of Naproxen derivatives.

Comp.	MlogP	S + logP	S + logD	MWt	M_NO	T_PSA	HBDH
4a	3.982	3.881	3.879	397.474	5	62.39	3
4b	3.982	3.874	3.873	397.474	5	62.39	3
4c	3.982	3.837	3.836	397.474	5	62.39	3
4d	4.574	4.716	4.713	448.373	5	62.39	3
4e	4.574	4.745	4.742	448.373	5	62.39	3
4f	4.574	4.772	4.77	448.373	5	62.39	3
5a	4.306	5.112	3.63	379.458	4	39.94	0
5b	4.306	5.023	3.587	379.458	4	39.94	0
5c	4.306	4.874	3.55	379.458	4	39.94	0
5d	4.897	5.989	4.434	430.358	4	39.94	0
5e	4.897	6.047	4.401	430.358	4	39.94	0
5f	4.897	5.951	4.149	430.358	4	39.94	0
6a	4.735	5.293	5.293	407.513	4	39.94	0
6b	5.316	6.317	6.317	458.412	4	39.94	0
6c	4.945	5.648	5.648	421.54	4	39.94	0
6d	5.52	6.653	6.653	472.439	4	39.94	0
7a	4.598	4.507	4.507	363.394	5	60.18	1
7b	4.598	4.525	4.525	363.394	5	60.18	1
7c	4.598	4.48	4.48	363.394	5	60.18	1
7d	4.922	5.312	5.312	414.293	5	60.18	1
7e	4.922	5.32	5.32	414.293	5	60.18	1
7f	4.922	5.377	5.377	414.293	5	60.18	1
8a	4.168	5.094	5.094	379.458	4	47.04	1
8b	4.168	5.111	5.111	379.458	4	47.04	1
8c	4.168	5.056	5.056	379.458	4	47.04	1
8d	4.491	5.886	5.886	430.358	4	47.04	1
8e	4.491	5.88	5.88	430.358	4	47.04	1
8f	4.491	5.934	5.934	430.358	4	47.04	1

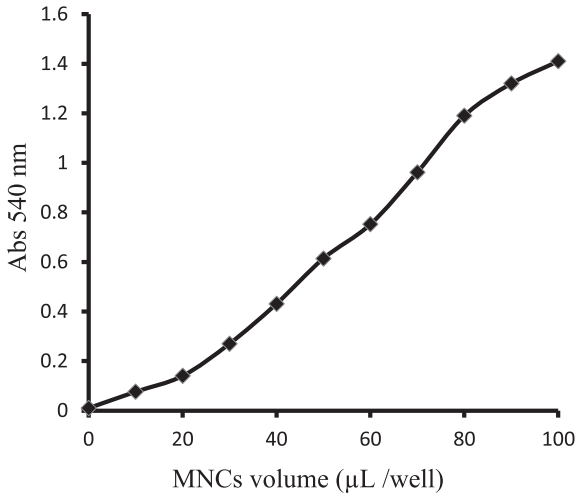

Fig. 3 MTT assay standard curve of volume of MNCs vs absorbance.

oxadiazoles **7a-f** were found second most active series among naproxen derivatives in which the most potent compounds were **7a** (IC_{50} 1.72 ± 0.54 µM) and **7c** (IC_{50} 3.75 ± 0.65 µM), while all the remaining compounds of this series also showed excellent activity in the range of 13.12 ± 0.41 µM – 42.85 ± 0.58 µM. Then the third most active series was thiosemicarbazides **4a-f**, in which compounds appeared in potent to moderate inhibition in the range of IC_{50} 1.13 ± 0.62–91.12 ± 0.48 µM while two compounds **4a**, **4b** were found inactive. 2-Arylamino-5-substituted-1,3,4-thiadiazoles **8a-f** showed potent to poor inhibition, that appeared with inhibitory concentration value of IC_{50} at the range of IC_{50} 1.23 ± 0.35 µM – 123.47 ± 0.37 µM, respectively, while compound **8b** was found inactive.

3.2.2. In vitro α-glucosidase studies

Naproxen derivatives were also evaluated for their *in vitro* α-glucosidase inhibitory potential. The results are summarized in Table 2. The results showed that these compounds exhibited significant α-glucosidase inhibitory activity (IC_{50} 1.0 ± 1.13 µ

Table 4 Binding energies and different types of binding interactions of naproxen derivatives within the active pocket of 15-LOX.

Comp.	Binding Energy (kJ/mol)	Hydrophobic Interactions	Hydrogen Bond Interactions	Other Interactions
4e	−33.2956	Phe108 (π- π stacked), Leu120 (π-alkyl), Leu246 (π-alkyl), Trp286 (π-alkyl), Arg533 (alkyl), His515 (alkyl), Trp772 (alkyl), Arg767 (alkyl), Glu244 (Attractive Charge)	————	Asn128, Asn534, Val511, Thr529, Tyr525, Val126, Asn169, Gly247 (Van der waals)
4f	−30.0616	Val126 (alkyl), Val520 (alkyl), Leu246 (π-alkyl), Trp130 (π-alkyl), Phe108 (π-alkyl)	Asp768 (H-bond donor)	Lys526 (π-cation), Thr529 (π-sulphur), Phe144, Leu521, Asn146, Tyr525, Arg767, Pro530, Arg533, Gly247, Arg242, Glu244, Asn128, His515, Trp772 (Van der waals)
5b	−30.2236	Arg182 (alkyl), Val520 (π-alkyl)	Tyr184 (C–H bond), Lys526 (C–H bond, Asp243 (C–H bond	His515 (π-cation), Leu169, Phe143, Asn128, Phe144, Leu521, Asn146, Thr529, Trp772, Arg767, Tyr525, Glu244, Pro241 (Van der waals)
6b	−32.298	His515 (alkyl), Arg533, Val762, (alkyl), Pro530 (π-alkyl), Lys526, Trp772, Phe143 (π-alkyl)	————	Asp768 (π-anion), Asn835, Thr529, Tyr532, Asp243, Cys127, Val520, Asn128, Tyr525, Arg767 (Van der waals)
6c	−31.0764	Thr529 (Amide- π stacked),Arg767 (alkyl), Trp772 (alkyl), Pro530 (alkyl), His515 (π-alkyl)	Asp768 (C–H bond)	Tyr532, Tyr525, Glu244, Val520, Tyr184, Arg141, Arg182, Asp243, Ser129, Lys526, Leu246 (Van der waals)
7a	−27.4104	Thr529 (Amide- π stacked),Arg767 (alkyl), Pro530 (alkyl), Lys526 (π-alkyl)	Asp768 (Conventional H-bond)	Arg533 (π-anion), Asn534, Leu246, Trp772, His515, Cys127, Val520, Phe143, Arg141, Arg182, Asn128, Asp243, Tyr525, Val762 (Van der waals)
7c	−28.0408	Val520 (alkyl), Tyr525 (alkyl), Lys526 (alkyl), Val762 (π-alkyl)	Arg533 (C–H bond), Val126 (Conventional H-bond)	Arg182 (π-anion), His515, Trp772, Thr529, Asn769, Asn835, Cys127, Phe143, Arg141, Ser129, Asp243 (Van der waals)
8c	−31.4348	Tyr532 (Amide- π stacked),Thr529 (Amide- π stacked) ,Val520 (alkyl), Val126 (alkyl), Trp772 (π-alkyl) , Pro530 (π-alkyl), Arg533 (π-alkyl)	Ala145 (C–H bond), Val126 (Conventional H-bond)	Lys526 (π-cation), Leu521, Asn146, Tyr525, His515, Leu246, Asn769 (Van der waals)
8d	−30.6068	Thr529 (Amide- π stacked),Glu165 (Halogen-bond), Trp772 (alkyl), Arg767 (alkyl), Pro530 (alkyl), Val520 (π-alkyl), Leu169 (π-alkyl)	———	Arg182, Asp243 (π-cation), Arg141 (π-anion), Leu246, Tyr525, His515, Tyr184, Asn128, Phe143, Glu244, Val762, Asn835, Asn769 (Van der waals)

M – 367.2 ± 1.23 μM) in comparison to the standard drug acarbose (IC_{50} 375.82 ± 1.76 μM) except compounds **5a**, **8b**, and **8d**, which were found inactive. Compounds **6c** (IC_{50} 1.0 ± 1.13 μM), **7c** (IC_{50} 1.1 ± 1.17 μM) and **7e** (IC_{50} 2.1 ± 1.12 μM) were the most potent ones among the series, followed by compounds **8c** (IC_{50} 24.3 ± 1.25 μM), **4e** (IC_{50} 47.5 ± 1.17 μM), and **4a** (IC_{50} 55.5 ± 1.12 μM), which were many folds better than the standard drug acarbose.

The structure activity relationship (SAR) has been established. The SAR was mainly based upon bringing about differences in azoles moiety and substituent pattern at phenyl ring. Thiosemicarbazides **4a-f** exhibited good inhibitory potential, in which the most active compounds were **4a** (IC_{50} 55.5 ± 1.12 μM), having fluoro substituent at 2-position at phenyl ring, while compound **4e** (IC_{50} 47.5 ± 1.17 μM), and **4f** (IC_{50} 67.3 ± 1.21 μM) having dichloro groups at 2,4 and 3,4-position, respectively. All other compounds of the same series appeared in the range of 121.6 ± 1.21–289.3 ± 1.13 μM. 5-Substituted-phenyl-4H-1,2,4-triazole-3-thiols **5a-f** and S-alkylated 1,2,4-triazoles **6a-d** showed potent to poor (IC_{50} 1.01 ± 1.13 μM to 340.14 ± 1.21 μM) inhibitory activity as compared to thiosemicarbazides **4a-f**. Compound **6c** (IC_{50} 1.01 ± 1.13 μM) was the potent inhibitor among this series. The most significant series among the synthesized compounds was 2-Arylamino-5-substituted-1,3,4-oxadiazoles **7a-f**, in which most of the compounds showed significant inhibitory potential (IC_{50} 1.1 ± 1.17 μM to 121.3 ± 1.13 μM). Compound **7c** (IC_{50} 1.1 ± 1.17 μM), and **7e** (IC_{50} 2.1 ± 1.12 μM), both appeared as potent inhibitors having fluoro substituent at 4 and dichloro at 2,4 position, respectively. 2-Arylamino-5-substituted-1,3,4-thiadiazoles **8a-f** also showed good to moderate IC_{50} 24.3 ± 1.25 μM to 367.2 ± 1.23 μM, inhibitory activity except compounds **8b** and **8e** that were inactive. The most potent compound among this series was compound **8c** (IC_{50} 24.3 ± 1.25 μM), having fluoro substituent at 4 position. These results suggests that those compounds with oxadiazole moiety were more potent than thiosemicarbazides, which were more active than triazole and thiadiazole containing compounds.

3.2.3. Cellular viability assay

The cytotoxicity of all synthesized naproxen derivatives was evaluated against mononuclear cells (MNCs) isolated from fresh blood. The percent viability of compounds was determined at 0.25 mM concentration as mentioned in the experimental section, and data is given in Table 2. Compounds **4a-f** exhibited 99.8 to 80.5% cellular viability, compounds **5a-f** showed 96.4 to 92.6% viability, and compounds **6a-d** showed 97.4 to 87.6% viability against MNCs. Likewise, compounds **8a-f** maintained cellular viability in the range of 89.6 to 67.4%. However, in compounds **7a-f,** two compounds **7d** and **7f** exhibited 63.7 % and 65.4 % cellular viability, respectively, while all the remaining compounds showed cell viability in the range of 98.5 to 73.6%. This technique is good agreement with the previous studies [63–74]. These values are even lesser than the standard cytotoxic drugs cyclophosphamide, cisplatin, and curcumin (Table 2). It also indicates that the most active compounds against the soybean 15-LOX enzyme, that is, **5a** (96.2%), **5b** (92.6%), **5c** (95.3%), and against α-glucosidase enzyme that is **7c** (98.5%) and **7e** (95.4%) were the least toxic. The data altogether suggests that azole derivatives of naproxen especially triazoles and oxadiazole inhibited 15-LOX and α-glucosidase enzymes in differentially in *in vitro* enzyme inhibition studies, and the active compounds, in general, were the least toxic towards MNCs.

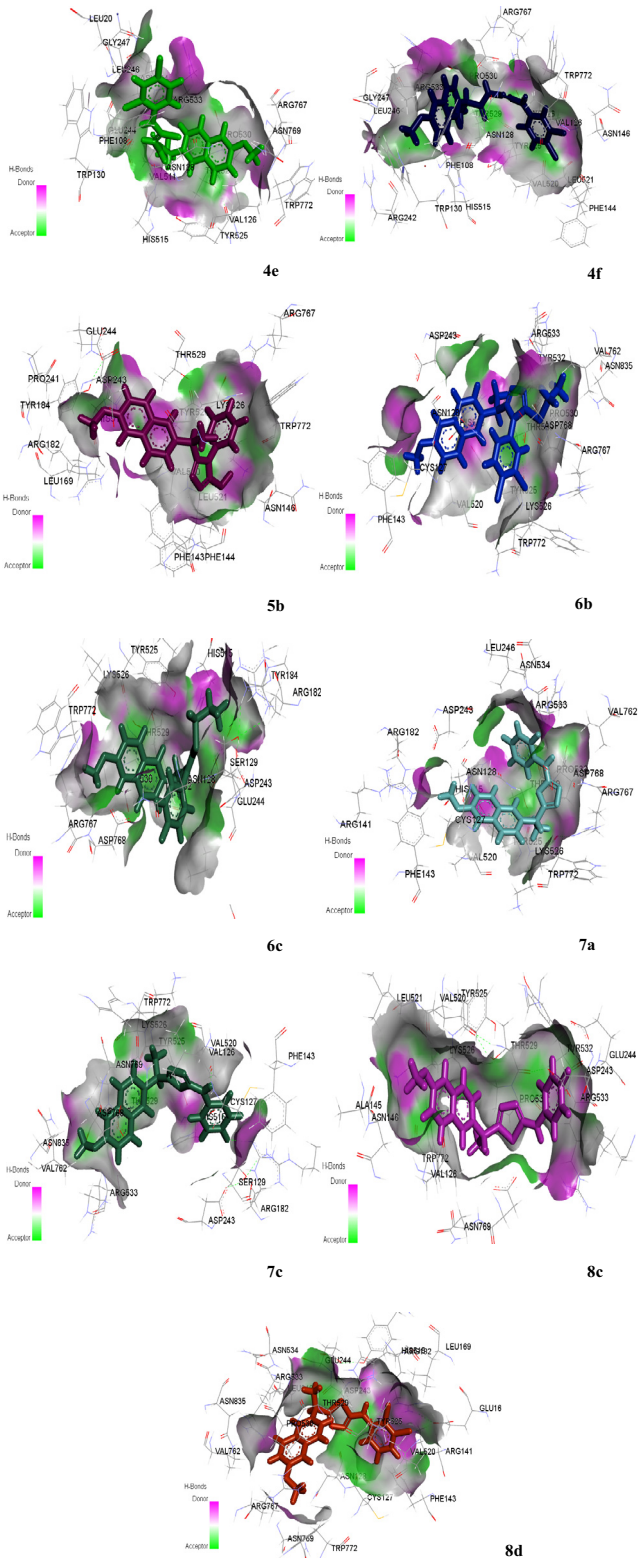

Fig. 4 3-D docking interactions of naproxen derivatives (4e, 4f, 5b, 6b, 6e, 7a, 7c, 8c, 8d) within the active pocket of 15-LOX.

Table 5 Binding energies and binding interactions of naproxen derivatives within the active pocket of α-glucosidase.

Comp.	Binding Energy (kJ/mol)	Hydrophobic Interactions	Hydrogen Bond Interactions	Other Interactions
4e	−29.88	Arg315, Tyr158 (π-alkyl) Pro312 (alkyl-alkyl)	Asp215, Ser240, Phe303, Asp352	Phe314, Leu313, Val216, Phe178, Ser157, Ser241 (Van der waals)
6c	−31.48	Ser241 (alkyl), Phe108 (π-alkyl)	Glu411, Asp307, Lys156, Ser240	Ser240, Tyr158 (π-anion), Phe314, Phe159, Phe178, Phe303, Pro312, Thr310, Thr316 (Van der waals)
7c	−27.08	Arg315 (alkyl), Asp215, Lys156 (π-alkyl)	Arg442	Val216 (π-cation), Leu169, Phe143, Asn128, Phe144, Leu521, Asn146, Thr529, Trp772, Arg767, Tyr525, Glu244, Pro241 (Van der waals)
8c	−28.92	Tyr158 (alkyl-alkyl), Asp352, Arg442, Leu314 (π-alkyl)	Glu277, Phe303	Val216, Pro312, Leu313, Phe178, Gln182, His112, Tyr72 (Van der waals)

3.2.4. *ADME studies*

In the search for lead molecules, the Med Chem Designer software version 3.0 was utilized to determine pharmacological ADME (absorption, distribution, metabolism, and excretion) investigations of the compounds (Table 3). These ADME properties are predicted by Lipinski's rule of five. This rule states that good drug absorption or permeation happens when at least three of the following factors are met: H-bond donors should be < 5; H-bond acceptors should be < 10; molecular weight should be < 500 Da; and log P should be < 5 [75]. Furthermore, the drug's polar surface area, rotatable bonds, and oral bioavailability are all linked. Orally accessible drugs have a polar surface area of < 140 Å^2 and rotatable bonds of < 10; the sum of hydrogen bond donor and acceptor (M_NO + HBDH) should be ≤ 12 [76]. LogP is used to determine lipophilicity. Its value of < 5.0 indicates that it will have an excellent partition coefficient. The octanol–water distribution coefficient, M logP, has a value of < 5 indicating that these molecules are drug-like. Drug bioavailability is predicted by larger logD and logP values, as well as a smaller number of

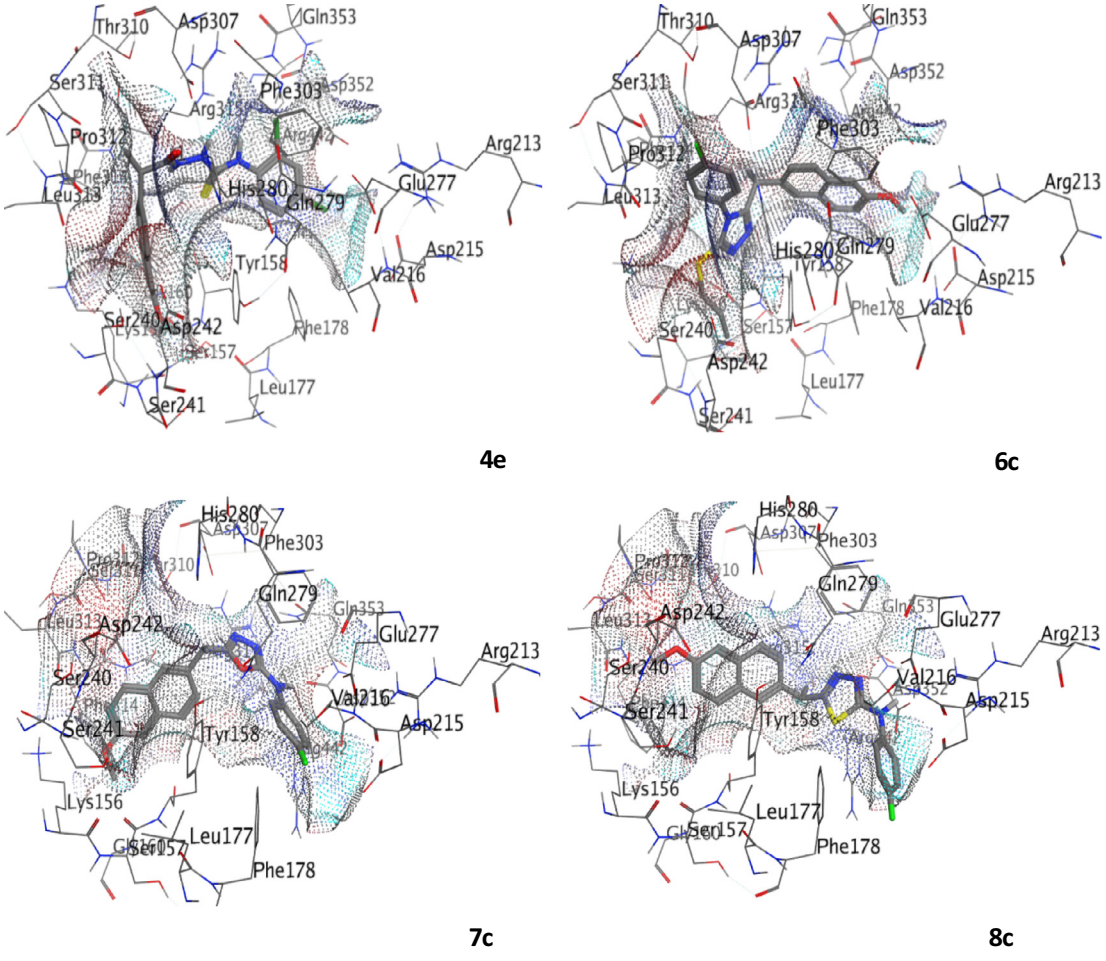

Fig. 5 3-D docking interactions of naproxen derivatives (4e, 6c, 7c, 8c) within the active pocket of α-glucosidase.

hydrogen bonds [77]. The data show that all of these compounds obey Lipinski and Veber's drug-likeness property tests [75,76].

Various volumes of MNCs were taken in wells and assay performed as mentioned in the text. A linear response was exhibited from 20 to 80 μL volume of cells. A volume of 20 μL MNCs was selected per assay. Assay was performed in triplicate. However, only representative graph is given in Fig. 3.

3.3. Molecular docking studies

3.3.1. 15-Lipoxygenase docking results

The most potent derivative from each respective series was selected for the molecular docking studies. It was observed that the results were found in accordance with the *in vitro* enzyme inhibition studies. The binding energies of the selected compounds are given in Table 4. All the derivatives showed better interactions within the active pocket and were found more potent compared to the standards. i.e., Baicalein −21.6772, Quercetin-25.01 kJ/mol.

Among the most potent derivatives, compound **4e** was found as the most potent derivative of 15-LOX with the binding score of –33.296 kJ/mol. These compounds formed bonding and non-bonding interactions including strong hydrogen bond interaction, alkyl interaction, π-alkyl interactions and Van der waals interactions. The 3D interactions are shown in the following Fig. 4.

3.3.2. α-Glucosidase docking results

The most potent derivative from each respective series was selected for the molecular docking studies. It was observed that the results were found in accordance with the *in vitro* enzyme inhibition studies. The binding energies of the selected compounds are given in Table 5**.**

Among the derivatives, compound **6c** was found as the most potent derivative of α-glucosidase with the binding score of −31.48 kJ/mol. These compounds formed bonding and non-bonding interactions including strong hydrogen bond interaction, alkyl interaction, π-alkyl interactions and Van der Waals interactions. The 3D interactions are shown in the following Fig. 5.

4. Conclusions

In conclusion, a new class of naproxen derivatives were conveniently synthesized and characterized. All these synthesized derivatives were further investigated for their dual enzyme inhibitory potential against the 15-LOX and α-glucosidase enzymes. Naproxen has been reported as an active 15-LOX inhibitor in our previous studies, and its derivatives, particularly compounds **4e**, **5a-c**, and **8c**, were found to be more potent as 15-LOX inhibitors in the current study. LOX results demonstrate that majority of the compounds produced potent LOX inhibitors using the highly sensitive screening chemiluminescence method rather than the UV approach. In the case of α-glucosidase inhibitory activity, all compounds exhibited inhibitory values lower than the reference drug acarbose, indicating that compounds **6c**, **7a**, **7c**, and **7e**, showed considerable inhibitory activity against α-glucosidase. SAR studies illustrated that in the case of 15-LOX, triazoles having flouro substituents at 2, 3, and 4 positions of the phenyl ring, and in the instance of α-glucosidase, oxadiazole with a flouro substituent at position 4 and a dichloro substituent at position 2,4 of the phenyl ring enhanced the inhibitory profile of these compounds. The most potent compounds retained the viability of blood MNCs, and *in silico* analysis affirmed the drug-ligand interactions. These findings collectively suggest that the active compounds with the lowest toxicity are potential 'lead' molecules for further studies in the development of LOX and α-glucosidase inhibitory molecules.

CRediT authorship contribution statement

Asma Sardar: Conceptualization, Writing – original draft. **Obaid-ur-Rahman Abid:** Conceptualization, Writing – original draft. **Saima Daud:** Conceptualization, Writing – original draft. **M. Fakhar-e-Alam:** Conceptualization, Writing – original draft. **Muhammad Hussnain Siddique:** Conceptualization, Writing – original draft. **Muhammad Ashraf:** Conceptualization, Writing – original draft. **Wardah Shahid:** Conceptualization, Writing – original draft. **Syeda Abida Ejaz:** Conceptualization, Writing – original draft. **M. Atif:** Writing – review & editing. **Shafiq Ahmad:** Writing – review & editing. **Sulman Shafeeq:** Writing – review & editing. **Muhammad Afzal:** Writing – review & editing.

Declaration of Competing Interest

The authors declare that they have no known competing financial interests or personal relationships that could have appeared to influence the work reported in this paper.

Acknowledgement

Researchers Supporting Project number (RSP-2021/397), King Saud University, Riyadh, Saudi Arabia.

References

[1] T. Grosser, E. Ricciotti, G.A. FitzGerald, The cardiovascular pharmacology of nonsteroidal anti-inflammatory drugs, Trends Pharmacol. Sci. 38 (8) (2017) 733–748.
[2] L.J. Crofford, Use of NSAIDs in treating patients with arthritis, Arthritis Res. Ther. 15 (S3) (2013).
[3] S.V. Bhandari, K.G. Bothara, M.K. Raut, A.A. Patil, A.P. Sarkate, V.J. Mokale, Design, synthesis and evaluation of antiinflammatory, analgesic and ulcerogenicity studies of novel S-substituted phenacyl-1,3,4-oxadiazole-2-thiol and Schiff bases of diclofenac acid as nonulcerogenic derivatives, Bioorg. Med. Chem. 16 (4) (2008) 1822–1831.
[4] N. Mamatha, N.S. Babu, K. Mukkanti, S. Pal, 2-(6-Methoxynaphthalen-2-yl) propionic acid (1,3-dimethylbutylidene) hydrazide, Molbank M741 (2011), https://doi.org/10.3390/M7411.
[5] D. Sarigol, A. Uzgoren-Baran, B.C. Tel, E.I. Somuncuoglu, I. Kazkayasi, K. Ozadali-Sari, O. Unsal-Tan, G. Okay, M. Ertan, B. Tozkoparan, Novel thiazolo[3,2-b]-1,2,4-triazoles derived from naproxen with analgesic/anti-inflammatory properties: Synthesis, biological evaluation and molecular modeling studies, Bioorg. Med. Chem. 23 (2015) 2518–2528.
[6] S. Abbas, S. Zaib, S. Ali, J. Iqbal, 15-LOX Inhibitors: Biochemical Evaluation of Flurbiprofen and its Derivaives, Life Sci. 1 (2020) 92–97, https://doi.org/10.37185/LnS.1.1.107.

[7] N. Kausar, S. Ullah, M.A. Khan, H. Zafar, Atia-tul-Wahab, M.I. Choudhary, S. Yousuf, Celebrex derivatives: Synthesis, α-glucosidase inhibition, crystal structures and molecular docking studies, Bioorg. Chem. 106 (2021) 104499.
[8] A. Mumtaz, J. Arshad, A. Saeed, M.A.H. Nawaz, J. Iqbal, Synthesis, Characterization and Urease inhibition studies of transition metal complexes of thioureas bearing ibuprofen moiety, J. Chil. Chem. Soc. 63 (2018) 3934–3940, https://doi.org/10.4067/s0717-97072018000203934.
[9] S. Ullah, M. Saeed, S.M.A. Halimi, M.I. Fakhri, K.M. Khan, I. Khan, S. Perveen, Piroxicam sulfonates biology-oriented drug synthesis (BIODS), characterization and anti-nociceptive screening, Med. Chem. Res. 25 (2016) 1468–1475, https://doi.org/10.1007/s00044-016-1571-5.
[10] P. Srivastava, K. Singh, M. Verma, S. Sivakumar, A.K. Patra, Photoactive platinum(II) complexes of nonsteroidal anti-inflammatory drug naproxen: Interaction with biological targets, antioxidant activity and cytotoxicity, Eur. J. Med. Chem. 144 (2018) 243–254, https://doi.org/10.1016/j.ejmech.2017.12.025.
[11] G. Mohiuddin, K.M. Khan, U. Salar, Kanwal, M.A. Lodhi, A. Wadood, M. Riaz, S. Perveen, Biology-Oriented Drug Synthesis (BIODS), In Vitro Urease Inhibitory Activity, and In Silico Study of S-Naproxen Derivatives, Bioorg. Chem. 83 (2019) 29–46.
[12] F. Seraj, Kanwal, K.M. Khan, A. Khan, M. Ali, R. Khalil, Z. Ul-Haq, S. Hameed, M. Taha, U. Salar, S. Perveen, Biology-oriented drug synthesis (BIODS), in vitro urease inhibitory activity, and in silico studies on ibuprofen derivatives, Mol. Diversity 25 (1) (2021) 143–157.
[13] I. Cacciatore, L. Marinelli, E. Fornasari, L. Cerasa, P. Eusepi, H. Türkez, C. Pomilio, M. Reale, C. D'Angelo, E. Costantini, A. Di Stefano, Novel NSAID-Derived Drugs for the Potential Treatment of Alzheimer's Disease, Int. J. Mol. Sci. 17 (7) (2016) 1035.
[14] A.R. Brash, Lipoxygenases: occurrence, functions, catalysis, and acquisition of substrate, J. Biol. Chem. 274 (1999) 23679–23682.
[15] J. Vinayagam, L.R. Gajbhiye, L. Mandal, M. Arumugam, A. Achari, P. Jaisankar, Substituted furans as potent lipoxygenase inhibitors: Synthesis, in vitro and molecular docking studies, Bioorg. Chem. 71 (2017) 97–101.
[16] R. Mashima, T. Okuyama, The role of lipoxygenases in pathophysiology; new insights and future perspectives, Redox Biol. 6 (2015) 297–310.
[17] F.-Q. Shen, Z.-C. Wang, S.-Y. Wu, S.-Z. Ren, R.-J. Man, B.-Z. Wang, H.-L. Zhu, Synthesis of novel hybrids of pyrazole and coumarin as dual inhibitors of COX-2 and 5-LOX, Bioorg. Med. Chem. Lett. 27 (16) (2017) 3653–3660.
[18] M.A. Abbasi, V.U. Ahmad, M. Zubair, M.A. Rashid, U. Farooq, S.A. Nawaz, M.A. Lodhi, T. Makhmoor, M.I. Choudhary, Atta-ur-Rahman, Benzoylsalireposide an anti-oxidant, lipoxygenase and chymotrypsin inhibitor, Proc. Pak. Acad. Sci. 42 (2005) 121–124.
[19] C. Hu, S. Ma, Recent development of lipoxygenase inhibitors as anti-inflammatory agents, Med. Chem. Comm. 9 (2) (2018) 212–225.
[20] M.N. Xanthopoulou, T. Nomikos, E. Fragopoulou, S. Antonopoulou, Antioxidant and lipoxygenase inhibitory activities of pumpkin seed extracts, Food Res. Int. 42 (5–6) (2009) 641–646.
[21] A.L. Tappel, The mechanism of the oxidation of unsaturated fatty acid catalyzed by hematin compounds, Arch. Biochem. Biophys. 44 (1953) 378–395.
[22] G. Alitonou, F. Avlessi, D. Sohounhloue, H. Agnaniet, J. Bessiere, C. Menut, Investigations on the essential oil of Cymbopogon giganteus from Benin for its potential use as an anti-inflammatory agent, Int. J. Aromather. 16 (1) (2006) 37–41.
[23] D. Kratky, A. Lass, P.M. Abuja, H. Esterbauer, H. Kühn, A sensitive chemiluminescence method to measure the lipoxygenase catalyzed oxygenation of complex substrates, BBA 1437 (1) (1999) 13–22.
[24] Y. Kondo, Y. Kawai, T. Miyazawa, H. Matsui, J. Mizutani, An assay for lipoxygenase activity by chemiluminescence, Biosci. Biotech. Biochem. 58 (2) (1994) 421–422.
[25] Y.S. Cho, H.S. Kim, C.H. Kim, H.G. Cheon, Application of the ferrous oxidation - xylenol orange assay for the screening of 5-lipoxygenase inhibitors, Anal. Biochem. 351 (1) (2006) 62–68.
[26] R.A. Pufahl, T.P. Kasten, R. Hills, J.K. Gierse, B.A. Reitz, R.A. Weinberg, J.L. Masferrer, Development of a fluorescence-based enzyme assay of human 5- lipoxygenase, Anal. Biochem. 364 (2) (2007) 204–212.
[27] W. Lu, X. Zhao, Z. Xu, N. Dong, S. Zou, X.u. Shen, J. Huang, Development of a new colorimetric assay for lipoxygenase activity, Anal. Biochem. 441 (2) (2013) 162–168.
[28] V. Pogaku, K. Gangarapu, S. Basavoju, K.K. Tatapudi, S.B. Katragadda, Design, synthesis, molecular modelling, ADME prediction and anti-hyperglycemic evaluation of new pyrazole-triazolopyrimidine hybrids as potent α-glucosidase inhibitors, Bioorg. Chem. 93 (2019) 103307.
[29] O. Simó-Servat, C. Hernández, R. Simó, Diabetic Retinopathy in the Context of Patients with Diabetes, Ophthalmic Res. 62 (2019) 211–217.
[30] V. Spallone, Update on the Impact, Diagnosis and Management of Cardiovascular Autonomic Neuropathy in Diabetes: What Is Defined, What Is New, and What Is Unmet, Diabetes Metab. J. 43 (2019) 3–30.
[31] K. Tziomalos, V.G. Athyros, Diabetic Nephropathy: New Risk Factors and Improvements in Diagnosis, Rev. Diabet. Stud. 12 (1-2) (2015) 110–118.
[32] P. Saeedi, I. Petersohn, P. Salpea, B. Malanda, S. Karuranga, N. Unwin, S. Colagiuri, L. Guariguata, A. A Motala, K. Ogurtsova, J. E. Shaw, D. Bright, R. Williams, IDF Diabetes Atlas Committee. Global and regional diabetes prevalence estimates for 2019 and projections for 2030 and 2045: Results from the International Diabetes Federation Diabetes Atlas, 9th edition. Diabetes Res Clin Pract. 2019 Nov; 157:107843. doi: 10.1016/j.diabres.2019.107843. Epub 2019 Sep 10. PMID: 31518657.
[33] G.J. Ye, T. Lan, Z.X. Huang, X.N.C.Y. Cheng, S.M. Cai, B.W. Ding, Design and synthesis of novel xanthone-triazole derivatives as potential antidiabetic agents: α-Glucosidase inhibition and glucose uptake promotion, Eur. J. Med. Chem. 177 (2019) 362–373.
[34] X. Zhang, G. Li, D. Wu, Y. Yu, N. Hu, H. Wang, X. Li, Y. Wu, Emerging strategies for the activity assay and inhibitor screening of alpha-glucosidase, Food Funct. 11 (2020) 66–82, https://doi.org/10.1039/c9fo01590f.
[35] G. Wang, Y. Peng, Z. Xie, J. Wang, M. Chen, Synthesis, α-glucosidase inhibition and molecular docking studies of novel thiazolidine-2,4-dione or rhodamine derivatives, MedChemComm 8 (2017) 1477–1484.
[36] M. Gollapalli, M. Taha, M. Tariq Javid, N. Barak Almandil, F. Rahim, A. Wadood, Y.A. Bamarouf, Synthesis of Benzothiazole Derivatives as a potent α-Glucosidase Inhibitor, Bioorg. Chem. 85 (2018) 33–48.
[37] H. Khan, M. Zafar, S. Patel, S.M. Shah, A. Bishayee, Pharmacophore studies of 1, 3, 4-oxadiazole nucleus: Lead compounds as α-glucosidase inhibitors, Food Chem. Toxicol. 130 (2019) 207–218.
[38] S. Akhter, S. Ullah, S. Yousuf, H.S. Atia-Tul-Wahab, M.I. Choudhary, Synthesis, crystal structure and Hirshfeld Surface analysis of benzamide derivatives of thiourea as potent inhibitors of α-glucosidase in-vitro, Bioorg. Chem. 107 (2021) 104531, https://doi.org/10.1016/j.bioorg.2020.104531.

[39] S. Shamim, K.M. Khan, N. Ullah, S. Chigurupati, A. Wadood, A. Ur Rehman, M. Ali, U. Salar, A. Alhowail, M. Taha, S. Perveen, Synthesis and Screening of (E)-3-(2-Benzylidenehydrazinyl)-5,6-diphenyl-1,2,4-triazine Analogs as Novel Dual Inhibitors of α-Amylase and α-Glucosidase, Bioorg. Chem. (2020) 103979, https://doi.org/10.1016/j.bioorg.2020.103979.

[40] H.A. Abuelizz, E.H. Anouar, R. Ahmad, N.I.I.N. Azman, M. Marzouk, R. Al-Salahi, Triazoloquinazolines as a new class of potent α-glucosidase inhibitors: in vitro evaluation and docking study, PLoS ONE 14 (2019) (2019) e0220379, https://doi.org/10.1371/journal.pone.0220379.

[41] Abbas al Mula, A Review: Biological Importance of Heterocyclic Compounds. Der Pharma Chemica, 9 (2017) 141-147.

[42] L. Yurttas, G.A. Ciftci, H.E. Temel, B.N. Saglik, B. Demir, S. Levent, Biological Activity Evaluation of Novel 1,2,4-Triazine Derivatives Containing Thiazole/Benzothiazole Rings, Anticancer Agents Med. Chem. 17 (2017) 1846–1853.

[43] S. Bajaj, V. Asati, J. Singh, P.P. Roy, 1,3,4-Oxadiazoles: An emerging scaffold to target growth factors, enzymes and kinases as anticancer agents, Eur. J. Med. Chem. 97 (2015) 124–141.

[44] M. Yusuf, P. Jain, Synthesis and biological significances of 1,3,4-thiadiazolines and related heterocyclic compounds, Arabian J. Chem. 7 (2014) 525–552.

[45] M. Malhotra, M. Sanduja, A. Samad, A. Deep, New oxadiazole derivatives of isonicotinohydrazide in the search for antimicrobial agents: Synthesis and in vitro evaluation, J. Serb. Chem. Soc. 77 (2012) 9.

[46] R.H. Tale, A.H. Rodge, A.P. Keche, G.D. Hatnapure, P.R. Padole, G.S. Gaikwad, S.S. Turkar, Synthesis and anti-bacterial, anti-fungal activity of novel 1,2,4-oxadiazole, J. Chem. Pharm. Res. 3 (2011) 496–505.

[47] B.K.S. Sadek, Fahelelbom, Synthesis, characterization, and antimicrobial evaluation of oxadiazole congeners, Molecules 16 (2011) 4339–4396.

[48] R. Mehmood, A. Sadiq, R.I. Alsanti, E.U. Mughal, M.A. Alsharif, N. Naeeem, A. Javid, M.M. Al-Rooqi, G.S. Chaudhry, S.A. Ahmad, Synthesis and Evaluation of 1,3,5-Triaryl-2-Pyrazoline Derivatives as Potent Dual Inhibitors of Urease and α-Glucosidase Together with Their Cytotoxic, Molecular Modeling and Drug-Likeness Studies, ACS Omega 7 (2022) 3775–3795, https://doi.org/10.1021/acsomega.1c06694.

[49] W. Shahid, M. Ashraf, M. Saleem, B. Bashir, S. Muzaffar, M. Ali, A. Kaleem, H. Aziz-Ur-Rehman, K. Amjad, N.R. Bhattarai, Exploring phenylcarbamoylazinane-1,2,4-triazole thioethers as lipoxygenase inhibitors supported with in vitro, in silico and cytotoxic studies, Bioorg. Chem. 115 (2021) 105261, https://doi.org/10.1016/j.bioorg.2021.105261.

[50] S. Muzaffar, W. Shahid, N. Riaz, M. Saleem, M. Ashraf, B. Aziz-ur-Rehman, A. Bashir, M. Kaleem, B. Al-Rashida, K. Baral, H.G. Bhattarai, Probing phenylcarbamoylazinane-1,2,4-triazole amides derivatives as lipoxygenase inhibitors along with cytotoxic, ADME and molecular docking studies, Bioorg. Chem. 107 (2021) 104525, https://doi.org/10.1016/j.bioorg.2020.104525.

[51] B. Bashir, W. Shahid, M. Ashraf, M. Saleem, Aziz-ur-Rehman, S. Muzaffar, M. Imran, H. Amjad, K. Bhattarai, N. Riaz. Identification of phenylcarbamoylazinane-1,3,4-oxadiazole amides as lipoxygenase inhibitors with expression analysis and in silico studies, Bioorganic Chemistry, 115 (2021)105243. https://doi.org/10.1016/j.bioorg.2021.105243.

[52] F. Chaudhry, W. Shahid, M. al-Rashida, M. Ashraf, M. A. Munawar, M. A.Khan, Synthesis of imidazole-pyrazole conjugates bearing aryl spacer and exploring their enzyme inhibition potentials, Bioorganic Chemistry, 108, 2021, 104686, https://doi.org/10.1016/j.bioorg.2021.104686.

[53] W. Shahid, S.A. Ejaz, M. Al-Rashida, M. Saleem, M. Ahmed, J. Rahman, N. Riaz, M. Ashraf, Identification of NSAIDs as lipoxygenase inhibitors through highly sensitive chemiluminescence method, expression analysis in mononuclear cells and computational studies, Bioorg. Chem. 110 (2021) 104818.

[54] S. Daud, OuR. Abid, A. Sardar, B. A. Shah, M. Rafiq, A. Wadood, M. Ghufran, W. Rehman, Z. Wahab, F. Iftikhar, R. Sultana, H. Daud, B. Niaz, Design, synthesis, in vitro evaluation, and docking studies on ibuprofen derived 1,3,4-oxadiazole derivatives as dual α-glucosidase and urease inhibitors. Med. Chem. Res. 31(2022)316-336. https://doi.org/10.1007/s00044-021-02814-6.

[55] A.L. Tappel, The mechanism of the oxidation of unsaturated fatty acids catalyzed by hematin compounds, Arch. Biochem. Biophys. 44 (1953) 378–395.

[56] D. Kratky, A. Lass, P.M. Abuja, H. Esterbauer, H. Kühn, A sensitive chemiluminescence method to measure the lipoxygenase catalyzed oxygenation of complex substrates, BBA 1437 (1) (1999) 13–22.

[57] M. Taha, S.A.A. Shah, M. Afifi, S. Imran, S. Sultan, F. Rahim, K.m. Khan, Synthesis, α-glucosidase inhibition and molecular docking study of coumarin based derivatives, Bioorg. Chem. 77 (2018) 586–592.

[58] J.C. Stockert, R.W. Horobin, L.L. Colombo, A. Blázquez-Castro, Tetrazolium salts and formazan products in cell biology: Viability assessment, fluorescence imaging, and labeling perspectives, Acta Histochem. 120 (2018) 159–167.

[59] S.Y. Al-nami, E. Aljuhani, I. Althagafi, H.M. Abumelha, T.M. Bawazeer, A.M. Al-Solimy, Z.A. Al-Ahmed, F. Al-Zahrani, N. El-Metwaly, Synthesis and Characterization for new nanometer Cu (II) complexes, conformational study and molecular docking approach compatible with promising in vitro screening, Arabian J. Sci. Eng. 46 (2021) 1365–1382.

[60] M.F. Ahmed, E.Y. Santali, R. El-Haggar, Novel piperazine–chalcone hybrids and related pyrazoline analogues targeting VEGFR-2 kinase; design, synthesis, molecular docking studies, and anticancer evaluation, J. Enzyme Inhib. Med. Chem. 36 (2021) 307–318.

[61] M. H. Mahnashi, B.A. Alyami, Y.S. Alqahtani, M.S. Jan, U. Rashid, A. Sadiq, A. O. Alqarni, Phytochemical profiling of bioactive compounds, anti-inflammatory and analgesic potentials of Habenaria digitata Lindl.: Molecular docking based synergistic effect of the identified compounds. J. Ethnopharmacol. 273 (2021) 113976.

[62] F. Chaudhry, W. Shahid, M. al-Rashida, M. Ashraf, M. A. Munawar, M. A. Khan, Synthesis of imidazole-pyrazole conjugates bearing aryl spacer and exploring their enzyme inhibition potentials. Bioorganic Chemistry, 108(2021)104686. doi:10.1016/j.bioorg.2021.104686.

[63] M. Atif, S. Firdous, R. Mahmood, M. Fakhar-e-Alam, S.S.Z. Zaidi, R. Suleman, M. Ikram, M. Nawaz, Cytotoxic and photocytotoxic effect of Photofrin® on human laryngeal carcinoma (Hep2c) cell line, Laser Phys. 21 (2011) 1235–1242, https://doi.org/10.1134/s1054660x11130020.

[64] M. Atif, S. Firdous, A. Khurshid, L. Noreen, S.S.Z. Zaidi, M. Ikram, In vitro study of 5-aminolevulinic acid-based photodynamic therapy for apoptosis in human cervical HeLa cell line, Laser Phys. Lett. 6 (2009) 886–891, https://doi.org/10.1002/lapl.200910087.

[65] M. Atif, M. Fakhar-E-Alam, S. Firdous, S.S.Z. Zaidi, R. Suleman, M. Ikram, Study of the efficacy of 5-ALA mediated photodynamic therapy on human rhabdomyosarcoma cell line (RD), Laser Phys. Lett. 7 (2010) 757–764, https://doi.org/10.1002/lapl.201010061.

[66] M.S. AlSalhi, M.H. Aziz, M. Atif, M. Fatima, F. Shaheen, S. Devanesan, W. Aslam Farooq, Synthesis of NiO nanoparticles and their evaluation for photodynamic therapy against HeLa

cancer cells, J. King Saud Univ. - Sci. 32 (2020) 1395–1402, https://doi.org/10.1016/j.jksus.2019.11.033.

[67] M. Fakhar-e-Alam, M. Aseer, M.S. Rana, M. Hammad Aziz, M. Atif, N. Yaqub, W.A. Farooq, Spectroscopic features of PHOTOGEM® in human Rhabdomyosarcoma (RD) cellular model, J. King Saud Univ. - Sci. 32 (2020) 3131–3137, https://doi.org/10.1016/j.jksus.2020.08.025.

[68] M. Atif, S. Iqbal, M. Fakhar-e-Alam, Q. Mansoor, K.S. Alimgeer, A. Fatehmulla, A. Hanif, N. Yaqub, W.A. Farooq, S. Ahmad, H. Ahmad, Y. ming Chu, Manganese-doped cerium oxide nanocomposite as a therapeutic agent for MCF-7 adenocarcinoma cell line, Saudi, J. Biol. Sci. 28 (2021) 1233–1238, https://doi.org/10.1016/j.sjbs.2020.12.006.

[69] M. Fakhar-e-Alam, M. Aqrab-ul-Ahmad, K.S. Atif, M.S. Alimgeer, N. Rana, W.A. Yaqub, H.A. Farooq, Synergistic effect of TEMPO-coated TiO2 nanorods for PDT applications in MCF-7 cell line model, Saudi, J. Biol. Sci. 27 (2020) 3199–3207, https://doi.org/10.1016/j.sjbs.2020.09.027.

[70] S. Iqbal, M. Fakhar-e-Alam, K.S. Alimgeer, M. Atif, A. Hanif, N. Yaqub, W.A. Farooq, S. Ahmad, Y.M. Chu, M. Suleman Rana, A. Fatehmulla, H. Ahmad, Mathematical modeling and experimental analysis of the efficacy of photodynamic therapy in conjunction with photo thermal therapy and PEG-coated Au-doped TiO2 nanostructures to target MCF-7 cancerous cells, Saudi, J. Biol. Sci. 28 (2021) 1226–1232, https://doi.org/10.1016/j.sjbs.2020.11.086.

[71] M. Atif, A.R. Malik, M. Fakhar-e-Alam, S.S. Hayat, S.S.Z. Zaidi, R. Suleman, M. Ikram, In vitro studies of Photofrin® mediated photodynamic therapy on human rhabdomyosarcoma cell line (RD), Laser Phys. 22 (2012) 286–293, https://doi.org/10.1134/s1054660x11230010.

[72] M. Atif, M. Fakhar-E-Alam, N. Abbas, M.A. Siddiqui, A.A. Ansari, A.A. Al-Khedhairy, Z.M. Wang, In Vitro Cytotoxicity of Mesoporous SiO2@Eu(OH)3 Core-Shell Nanospheres in MCF-7, J. Nanomater. 2016 (2016), https://doi.org/10.1155/2016/7691861.

[73] M. Atif, S. Iqbal, M. Fakhar-E-Alam, M. Ismail, Q. Mansoor, L. Mughal, M.H. Aziz, A. Hanif, W.A. Farooq, Manganese-Doped Cerium Oxide Nanocomposite Induced Photodynamic Therapy in MCF-7 Cancer Cells and Antibacterial Activity, Biomed Res. Int. 2019 (2019), https://doi.org/10.1155/2019/7156828.

[74] M. Fakhar-e-Alam, Z. Shafiq, A. Mahmood, M. Atif, H. Anwar, A. Hanif, N. Yaqub, W.A. Farooq, A. Fatehmulla, S. Ahmad, A.E.E. Abd Elgawad, K.S. Alimgeer, T.N. Gia, H. Ahmed, Assessment of green and chemically synthesized copper oxide nanoparticles against hepatocellular carcinoma, J. King Saud Univ. - Sci. 33 (2021), https://doi.org/10.1016/j.jksus.2021.101669 101669.

[75] C. Lipinski, F. Lombardo, B. Dominy, P. Feeney, Experimental and computational approaches to estimate solubility and permeability in drug discovery and development settings, Adv. Drug Del. Rev. 23 (1997) 4–25.

[76] D.F. Veber, S.R. Johnson, H.Y. Cheng, B.R. Smith, K.W. Ward, K.D. Kopple, Molecular properties that influence the oral bioavailability of drug candidates, J. Med. Chem. 45 (2002) 2615–2623.

[77] M. J. Waring Lipophilicity in drug discovery. Expert Opin. Drug Discov. 5 (2010) 235-238.